DEPARTMENT OF THE INTERIOR

U.S. GEOLOGICAL SURVEY

CRUISE REPORT,
Hawaiian GLORIA Cruise
F12-89-HW

by

Michael E. Torresan[1], David A. Clague[1], and Colin L. Jacobs[2]

Open-File Report 91-127

This report is preliminary and has not been reviewed for conformity with U.S. Geological Survey editorial standards (or with the North American Stratigraphic Code). Any use of trade, product, or firm names is for descriptive purposes only and does not imply endorsement by the U.S. Government.

[1]U.S. Geological Survey
  345 Middlefield Road, MS-999
  Menlo Park, CA   94025

[2]IOS
  Wormley, Godalming,
  Surrey, United Kingdom

1991

Summary of Scientific Results

1. The Murray Fracture Zone crosscuts the northwest corner of the survey area. The Fracture Zone consists of three major and a number of minor faults, all oriented about 255-258°. Deep sedimentary basins containing up to 0.8 sec of sediment lie between the ridges defining the Fracture Zone.

2. The horst-graben fabric produced at the East Pacific Rise some 90-95 Ma occurs on and north of the Hawaiian Arch. The horsts are spaced 1-2 km apart, have relief of up to 150 m, and are oriented about 350°. A small region within 100 km of the axis of the Hawaiian Ridge has dark and bright backscatter bands parallel to the horst-graben fabric, but no surface relief. The bands are possibly caused by either distinct sediment types overlying buried horsts and grabens, or differential compaction of the same sediment facies.

3. Five distinct seamount types occur in the area: 1) large flat-topped Hawaiian-type volcanoes 2) large, rough-surfaced non-circular Cretaceous seamounts 3) small rough-surfaced, nearly circular Cretaceous seamounts 4) small, smooth, circular, Cretaceous seamounts, and 5) 1-2 km diameter, high-backscatter, probable Late Tertiary seamounts on the Hawaiian Arch.

4. Six Cretaceous Ridges occur in the eastern part of the survey area; they are oriented 257°, approximately parallel to trend of the Murray Fracture Zone imaged on this survey.

5. The Hawaiian Arch fault zone is a series of up to 100-km-long south-facing scarps trending roughly 295° and located adjacent to a large seamount on the Hawaiian flexural arch near 25°40'N, 164°20' W. The faults apparently postdate the horst-graben structure of the Cretaceous seafloor, and likely result from tension associated with flexure of the arch.

6. Sediment distribution is controlled by proximity to the Hawaiian Ridge. The thickest units are located in the moat adjacent to the ridge and the total section thins away from the ridge and up the arch. Most of the survey area is covered by a drape of transparent sediment that we infer to be pelagic and hemipelagic sediment. The transparent section ranges up to 30 m in thickness and generally overlies a discontinuously-stratified unit that we infer to be turbidites. This laminated unit almost certainly formed in response to the more active growing phases of this portion of the Hawaiian Ridge. Based on the extensive and

nearly continuous nature of the transparent drape we suspect that turbidite sedimentation plays a minor role in present day sedimentation.

7. Nine small to moderate-sized debris avalanches were imaged during this survey. The debris avalanches are covered by 25 to 35 meters of transparent and laminated sediment which suggests that the slides are older than those located around the principal Hawaiian Islands. Buried blocks associated with a laminated unit of turbidite origin suggest that the slides and the turbidites are contemperaneous, and occurred during the active island growth phase.

8. Areas of apparent bedforms or more likely buried debris avalanche deposits occur in the Hawaiian Trough between regions of exposed blocky debris avalanches. One apparent field is located near 23°30'N, 163°6.5'W and covers an area of about 1300 km sq.

9. The northeastern margin of the St. Rogatien Bank edifice is a rotational slump with a number of large coherent blocks that have slid up to 35 km from their apparent source.

10. A possible 75-km long sediment gravity deposit (turbidite?) occurs north of Necker Island.

11. Shoal areas of the Hawaiian Ridge are characterized by gullies and canyons, possibly carved during lower stands of sea level. These are probably important conduits for the movement of coarser sediment downslope and into the surrounding Hawaiian Trough.

12. Three arcuate submerged carbonate reefs fringe the north side of Necker Island; another single carbonate reef fringes the north rift zone of St. Rogatien Bank. These carbonate reefs may be bryozoan-algal reefs formed about 10 Ma when sea surface temperatures were only marginal for coral growth.

INTRODUCTION

Cruise F12-89-HW ,3 November-26 November 1989, was the eighth survey in a multi-year program designed to image the Hawaiian Island EEZ using GLORIA, a long-range side-looking sonar. The objective of this program is to produce atlases showing the geologic and morphologic features of the seafloor so as to better evaluate the economic potential, geologic hazards, and other possible uses of the Hawaiian EEZ.

Cruise F12-89-HW followed F6-88-HW and F10-88-HW that were carried out in May and October 1988 (Torresan et al., 1989, and McGregor et al., 1989). A subsequent sampling or "ground truthing" leg F11-88-HW was conducted in October-November of 1988 (Clague et al., 1989). The 1988 legs completed coverage of the EEZ areas west to Necker Island on the south side of the chain and to Nihoa Island on the north side of the chain. Figures 1 and 2 provide geographic reference and trackline coverage for the area covered by this survey. The area surveyed is on the north side of the Hawaiian Ridge between Nihoa Island and St. Rogatien Bank. The remaining territorial waters of the Hawaiian EEZ will be imaged prior to January 1992.

In addition to collecting GLORIA data, operations include collecting two-channel seismic-reflection profiles using an air-gun sound source, 3.5 kHz high-resolution profiling, 10 kHz bathymetric echo-sounding, magnetic and gravity potential-field measurements, and upper water column temperature profiles using expendable bathythermographs.

OPERATIONS

The GLORIA surveys are conducted from the R/V Farnella, a converted freezer-trawler that is under lease to the U.S. Geological Survey through the Institute for Oceanographic Sciences (IOS) in Wormley, England. GLORIA surveying responsibilities are split between USGS and IOS personnel. IOS personnel are responsible for all operations involving GLORIA, deck operations, and maintenance of the seismic reflection and 3.5- and 10 kHz profiling systems. They are also responsible for the GLORIA watchstanding, and the ABC navigation and data logging system. The USGS personnel are responsible for monitoring the gravity meter, magnetometer, the seismic reflection, and the 3.5-

and 10 kHz recording systems. USGS personnel are also responsible for the real-time navigation, and the co-chief scientists (both USGS and IOS) are responsible for cruise planning, production of two field mosaics of the GLORIA data, and a preliminary science report.

The scientific and ship personnel are listed below. The personnel list is followed by a schedule of field operations and a review of the equipment employed during the survey.

SCIENTIFIC STAFF FOR F12-89-HW

U.S. Geological Survey

David A. Clague	Co-Chief Scientist/Geologist
Michael E.Torresan	Co-Chief Scientist/Geologist
Kaye Kinoshita	Navigator/DAFE/Watchstander
Dennis Mann	Geophysicist/Watchstander
William Weber	Geologist/Watchstander
Larry Kooker	Electronic Technician

Institute of Oceanographic Sciences, U.K.

Colin L. Jacobs	Co-Chief Scientist/Geologist
Derek Bishop	GLORIA Chief/Engineer
Derek Lewis	Navigator/Computer Tech
Robin Bonner	Engineer
Andrew Webb	Engineer
Robert E. Kirk	GLORIA Engineer

Guest Scientist

Timothy Francis	Geophysical Consultant

JMarr (Ships Crew)

John Cannan	Captain
Ronald Holliday	Chief Officer
Ashley Robinson	2nd Officer
Matthew Gilby	Chief Engineer
David Rogerson	2nd Engineer
Roger Keys	3rd Engineer
Robin Searle	Electrician
Alan Thompson	Bosun
Jimmy Springall	Seaman
Peter Appleyard	Seaman
Michael Jessop	Seaman
David Hill	Chief Cook
Mark Howard	2nd Cook
David Graves	Steward

Summary of Field Operations

The following list starts with the Julian day/Greenwich Mean Time (JD/GMT), for the starting point of the major survey segments of F12-89-HW. When converting to local time note that the day 307 is November 3, and that GMT is 10 hours ahead of local Hawaii time, eg., 1900 GMT is 0900 local. Figure 1 provides a geographic reference for the region covered by this survey and figure 2 is a trackline summary to provide a reference for the various stages of the survey.

Day 307 (Friday, November 2)
    1900: Sailed from Honolulu.
    2100: Launched P.E.S. and 3.5 kHz fish to collect transit bathymetry.

Day 308 (Saturday, November 3)
    1900: Arrived at launch point. Winds and seas high. Commenced
        launch of GLORIA vehicle and geophysical gear.

Day 309 (Sunday, November 4)
    0126: Start line 1 on course 305° to tie in with F-10-88 leg, imaging the
    inboard portion of the survey along the chain, through line 5 ending on
    310/2015.

Day 310 (Monday, November 5)
    2115: Start the standard GLORIA tracking pattern of long 290°/110° lines
    (even numbered lines) that ties our survey to the F6-88-HW survey on the
    northern side of the chain. This trackline pattern is continued through
    line 30 ending on 328/2100, and completes the quad to163°00'W, and
    the F12-89-HW GLORIA survey. All odd numbered lines are tie lines
    lines are tie lines oriented at about 000°.

Day 328 (Friday, November 24)
    2100: End line 30 and the GLORIA portion of the F12-89-HW
    survey. Retrieve all gear and steam for line 31 to begin geophysical
    survey across an unnamed seamount, and a survey of the north Kauai
    debris avalanche, imaged during F6-88-HW. While underway we

replace both the GLORIA cable and two stretch sections of the two-channel streamer.

Day 329 (Saturday, November 25)
0710: Start line 31, a bathymetric survey of a seamount imaged on F6-88-HW. Line ends on 329/1838.
1950: Start line 32, a survey of the north Kauai debris avalanche ending at 330/0338.

Day 330 (Sunday, November 26)
0338: End line 32, retrieve all gear and steam for Honolulu.
1900: Arrive Honolulu; end F12-89-HW Cruise.

Equipment Summary

This section summarizes problems encountered with the shipboard data collection systems. Appendix I (from Torresan et al., 1989) summarizes the standard operational procedures that were established for the 1986 surveys (Holmes et al., 1986; Normark et al., 1987 and 1989). Complete reviews of the trouble-shooting and repairs for each system are available in the electrical technicians' report.

Gravity Meter
The gravity meter, a LaCoste and Romberg S-53, functioned continuously for the entire cruise. The stabilizing shockcords were replaced due to wear at 0740 on JD 324. The signal may be unusually noisy for some undetermined time before this repair was completed. A gravity tie was established at pier 13 in Honolulu prior to departure. This gravity tie was remeasured following the cruise so that a drift correction could be applied to the data.

Magnetometer
The magnetometer was deployed following the streaming of all seismic gear (about 307/0100). Official logging began at 307/2300. The data are recorded on both strip-chart and magnetic tape, with the same recorder used for the gravity meter. There were no problems with the system. The Magnetometer was recovered prior to recovering the GLORIA fish on 328/2210 and then rede-

ployed at 328/2252. Final recovery occurred on 330/0338, following a short survey off northern Kauai.

Expendable Bathythermographs (XBT's)

The XBT probes were deployed daily, beginning on JD 310, to measure the thickness and temperature of the surface mixed layer, and the temperature profile of the thermocline. T-4 probes are capable of profiling to 460 m, and T-7 XBT's can profile to 760 m. T-7 probes were deployed weekly and T-4 probes were used on the other days. The system is interfaced to a computer that handles recording, plotting, formatting and data transmission. Data transmission is accomplished via satellite. The system performed well, with some fouling of the wire in the towed seismic gear. The probe was launched on the lee side of the vessel, about 20' fore of the stern. The following list is a record of the location of daily XBT drops and their success rate.

Day	XBT	Depth Rating	Record Length	Latitude	Longitude
310	T-07	760 m	Full	24°40.9'N	167°08.1'W
311	T-04	460 m	Full	23°52.8'N	164°15.9'W
312	T-04	460 m	Partial (340 m)	23°54.4'N	163°32.8'W
313	T-04	460 m	Partial (175 m)	25°09.3'N	167°07.1'W
313	T-04	460 m	Partial (335 m)	25°00.3'N	167°10.2'W
315	T-04	460 m	Partial (145 m)	24°14.3'N	163°44.2'W
315	T-04	460 m	Partial (285 m)	24°21.0'N	163°28.4'W
316	T-07	760 m	Full	25°32.7'N	166°47.0'W
319	T-04	460 m	Partial (330 m)	24°52.7'N	163°59.9'W
320	T-04	460 m	Partial (130 m)	24°46.4'N	162°54.2'W
321	T-04	460 m	Full	25°56.4'N	165°26.3'W
322	T-07	760 m	Full	25°32.5'N	163°24.8'W
323	T-04	460 m	Full	26°43.0'N	166°51.5'W
324	T-04	460 m	Full	26°02.0'N	164°00.5'W
325	T-04	460 m	Full	26°18.1'N	163°56.3'W
326	T-07	760 m	Partial (279 m)	28°38.3'N	163°01.2'W
328	T-04	460 m	Partial (318 m)	26°23.3'N	163°18.7'W
329	T-04	460 m	Full	26°22.9'N	162°28.6'W

3.5-kHz High-Resolution Profiling System

The 3.5-kHz reflection tow fish was deployed on 307/1300. The system was operational and official logging commenced at 307/2124. The system performed well with only routine maintenance throughout the course of the cruise. Generally, record quality degrades in water depths greater than 4800 m, but we were able to collect good quality records to depths exceeding 5000 m. Late in the cruise the records became noisy and the towfish was pulled in on 325/1930. No problems were found, the fish was redeployed, and the noise disappeared. We assume that the towfish snagged a piece of debris that worked free during the recovery operation.

10-kHz Echo-Sounding System

The 10-kHz echo-sounding system employs a tow fish similar to that of the 3.5-kHz system, and was deployed on 307/1300. The system worked flawlessly, with down time restricted to routine maintenance, and blade and paper roll changes.

Two-Channel Seismic Reflection System

The two-channel seismic reflection system employs a 2600 cm^3 (160 in^3) air-gun sound source, coupled with an 800 m two-channel streamer (including a weighted stabilizing line). Two 50 m long active sections are towed about 500 to 600 m behind the air gun. The air gun is fired every 10 seconds. Data is recorded on a MASSCOMP computer, and a one-channel, six-second analog record is displayed on a Raytheon line scan recorder (LSR) and a CRT monitor. The memory function of the LSR was used to print the profile with a constant orientation (west and north end of the profile are on the left, east and south profiles are on the right) and to reduce vertical exaggeration. Vertical exaggeration is about 4:1 at a speed of about 8.5 knots.

The two-channel seismic reflection system performed well during the survey. The streamer and air gun were deployed by 308/2000, but official logging did not begin until 308/2200 because the GLORIA system required 5 hours to begin operating, owing to some electronic problems. The air guns required little attention aside from the routine swaps at 5 day intervals and, unlike previous Hawaiian legs, the Teledyne streamer required no attention. MASSCOMP hang-ups generally were not a problem and also required little attention. Alert watch keeping, and regular cleaning kept the system operational most of the time. The airgun and streamer were recovered prior to recovery of the GLORIA

fish on 328/2210 and then were redeployed on 329/1838 for a short survey of the landslide north of Kauai. Final recovery of the airgun and streamer occured at 330/0338.

Shipboard Positioning Systems

The shipboard positioning systems performed well. We were able to avoid most of the problems encountered during the first two 1986 GLORIA cruises (Holmes et al., 1986, and Normark et al., 1987) owing to the improved GPS network coupled with the addition of the real-time, rho-rho Loran positioning system. The new system (described in Normark et al., 1987) incorporates a real-time trackline display for the ships' bridge personnel, that displays ships position relative to the desired survey line.

The GPS system worked well, providing about 15 hours per day navigation. When GPS is unavailable, the rho-rho Loran C was used. The rho-rho performed erratically, especially when close to the baseline between station X and the north side of the islands. Many times we had to resort to both transit satillites and dead reckoning while waiting for a GPS update.

GLORIA Side-scan Sonar System

The deployment and operation of the GLORIA system is covered in extensive logs kept by the IOS personnel. More detailed summaries are available in Sommers et al., 1978, Laughton, 1981, and references therein. A summary of the GLORIA pass record and the number of files is presented in Appendix 2. Note that one pass equals 6 hours.

The GLORIA system was launched on about 308/1900 and operated well for the duration of the survey. Except for course changes, the system operated continuously until the termination of the survey on 328/2240.

GLORIA Shipboard Image Processing

The techniques employed in shipboard processing are described in detail in Normark et al., 1987 and 1989, and will not be elaborated upon here. No special shading techniques, such as those used by Normark et al., 1989, were applied. Following the printing of the GLORIA images, the images were laid down over corrected and smoothed navigation plots and mosaicked Interpretation of the images and preparation of an isopach map of 3.5 kHz penetration were done following the mosaicking.

RESULTS

Owing to the rather extensive existing coverage of the Hawaiian EEZ we will present this report as a series of topical sections guided by the results obtained previously during GLORIA surveys of the Hawaiian EEZ. We were fortunate to have onboard copies of previous cruise reports and a series of topical articles on the geology of the region, including many resulting from knowledge gained from the 1986 and 1988 GLORIA surveys and GLORIA ground truthing cruises. We were also had 1/375,000 scale prints of the mosaics produced from the last GLORIA surveys collected during May and September-October 1988, aboard cruises F6-88-HW and F10-88-HW, respectively.

The following outline organizes the topics addressed:

1. Cretaceous seafloor
       1a. Murray Fracture Zone
       1b. Seafloor spreading fabric
       1c. Seamount distribution and characteristics
       1d. Cretaceous ridges
       1e. The Hawaiian Arch fault zone
       1f. Magnetics

2. Sedimentation
       2a. Sediments and 3.5 kHz echo character
       2b. Sediment dispersal patterns and thickness
       2c. Apparent bedform fields

3. Island degradation: debris avalanches, slumps, and sediment gravity flows
       3a. Debris avalanches
       3b. Slumps
       3c. Sediment gravity deposits
       3d. Small scale mass wasting features (debris chutes and gullies)

4. Submerged carbonate reefs

1. Cretaceous seafloor

1a. Murray Fracture Zone

A small region of the Murray Fracture Zone (about 100 km and 175 km of the north and south sides respectively) was imaged in the extreme northwestern corner of the survey area (fig 3). The fracture zone consists of three major lineaments and several minor ones that are oriented about 255°-258°. South of the southern scarp face of the Murray Fracture Zone, the horst-graben fabric is strongly developed. Adjacent to the ridge that forms the southern trace of the Murray Fracture Zone, the northernmost 2-3 km of the horst-graben fabric bends towards the northeast. This southernmost ridge separates the horst-graben fabric to the south from a deep sedimentary basin to the north. This sedimentary basin is the southern most of two, and possibly three, fracture zone valleys that make up the Murray Fracture Zone. Sediment fill in this basin is at least 0.8 sec. In the center of the basin, a few basement highs project above the sediment; these presumably are the tops of another ridge within the Murray Fracture Zone complex. Northwest of the sediment filled fracture zone valley is a block that displays the horst-graben fabric seen outside the fracture zone. This block is 12 km wide to the southwest and 16 km wide to the northeast. Sediment gravity flows shed off this block into a fracture zone valley to the northwest. This second sedimentary basin contains less sediment than the one to the southeast, perhaps 0.6 sec, and is about 8 km wide to the northwest and 16 km wide to the southeast. The combined width of the fracture zone valleys and the block of horst-graben terrain is 24 km. The sedimentary basin has low-relief horst-graben fabric faintly exposed on the north side. This basin is bounded by a steep ridge and a block of horst-graben fabric seafloor, which becomes progressively buried by sediment to the northeast. Two central volcanoes occur within the sediment-filled basin. The northwesternmost trace of the Murray Fracture Zone occurs 25 km northwest of the steep ridge and across the sediment-filled basin. The combined width of the Murray Fracture Zone is about 80 km.

The Fracture Zone is located where earlier studies (Malahoff and Woollard, 1970), based mainly on elongate magnetic anomalies, suggested it would be. However, the models based on magnetic anomalies indicate only two major strands in the fracture zone, rather than the three seen by GLORIA. The orientation of the Murray Fracture Zone is not parallel to that of the Molokai

Fracture Zone to the east (Normark et al., 1989; Torresan et al., 1989), but is rotated counterclockwise about 10-15°.

1b. Seafloor spreading fabric

The horst-graben relief generated at the East Pacific Rise about 90-95 Ma is clearly imaged in the entire northern part of the survey area, and in a small region within about 100 km of the axis of the Hawaiian Ridge just east of St. Rogatien Bank (figs 3, 4, and 5). The tectonic fabric is oriented about 350°. Individual horsts can be traced for at least 50 km, although most are no more than 25-30 km long. The small region closest to the Hawaiian Ridge has a clear banding of dark and bright backscatter zones, but there is essentially no seafloor relief. The different bands of backscatter may be caused by either different sediment types overlying the horsts and the grabens, or differential compaction of the same sediment type. On the Hawaiian Arch and further to the north, the horst-graben dark-bright backscatter bands are caused mainly by topographic relief. The horsts are uplifted from 15-150 m above the grabens. Sediment is ponded in the grabens and thins over the horsts, particularly on their steep slopes. The horsts and grabens have irregular spacing ranging from <1 to perhaps 3 km; most are spaced about 1-2 km apart.

1c. Seamount distribution and characteristics

Five distinct types of seamounts occur in the surveyed region (figs 3 and 5): 1) large flat-topped seamounts that are part of the Hawaiian Ridge, 2) large (>10 km across) rough-surfaced non-circular seamounts, 3) small (5-10 km across) rough-surfaced seamounts, 4) small (generally 3-10 km across) circular low-relief seamounts with or without summit calderas, and 5) very small (<about 2 km across) high-backscatter rounded volcanic mounds that are located near the axis of the Hawaiian Arch.

The section of the Hawaiian Ridge imaged on this cruise extends from Nihoa Island to the southeast to St. Rogatien Bank on the northwest. Lava samples have been collected from Nihoa Island, Necker Island, and La Perouse Pinnacles (Dalrymple et al., 1974), and have been dredged from 6 locations along this section of the Ridge (Clague and Dalrymple, 1987). Rocks from 5 locations have been dated using K-Ar techniques. The ages of the volcanoes progressively increase from 7.2 Ma at Nihoa Island to 13 Ma at Brooks Bank (see age summary in Clague and Dalrymple, 1987). These volcanoes are dis-

tinctive on the GLORIA images because they are extremely large, flat-topped, and surrounded by landslide deposits. The upper slopes are commonly cut by canyons, and drowned carbonate reefs occur near the main break-in-slope at about 1500 m depth (fig 5). Submarine rift zones extend from many of the volcanoes; these are seen as steep regions of high irregular backscatter.

The second type of seamount is steep and rough surfaced. These volcanoes are commonly irregular in plan. An example is Chopin Seamount in the southern Musicians Seamounts. This seamount is a series of smaller overlapping volcanic edifices that combine to make an elongate volcanic seamount that is not oriented parallel to either the trend of fracture zones or seafloor horst-graben fabric. These seamounts are interpreted to be of Cretaceous age and to have formed soon after the ocean crust on which they are built.

The third group of seamounts are much smaller than the last group, cicular in plan, and rough-surfaced. These too are probably Cretaceous in age and formed on the seafloor soon after its creation at the East Pacific Rise some 90-95 Ma. Most of these occur in the Hawaiian Trough where the sediment may be quite thick; many of these volcanoes may be the tops of much larger edifaces.

The forth group of seamounts are small, round, low-relief volcanoes. They occur scattered throughout the survey area, occasionally grouped into chains. These volcanoes have steep slopes near their base, but rapidly flatten. On the GLORIA images they appear as a narrow band of high-backscatter around a low-backscatter, flat-topped central area. These volcanoes are similar in morphology to many of those studied on or adjacent to the East Pacific Rise (Fornari et al., 1989). We suspect that these formed at the East Pacific Rise, essentially at the same time the ocean crust was forming. A recent study of similar seamounts along the East Pacific Rise shows that many of these volcanoes occur in short chains that are parallel to either the direction of spreading (transform-parallel) or the direction of absolute plate motion (Batiza, 1990). We have examined the spatial relations of the small circular seamounts in the surveyed area and find four groups that are aligned in chains. Of these, two are subparallel to the fracture zone trend (262° and 265°), and the other two trend 230° and 278°. Clearly, these trends cannot both be the direction of absolute Pacific plate motion 90-95 Ma.

The fifth type of seamounts are small (a few km across), steep, and have high backscatter. They occur on or near the crest of the Hawaiian Arch, mainly in a group located northeast of the Hawaiian Arch Fault Zone. These volcanoes

are interpreted to be young and to have formed along the flexural arch as it grew in response to loading of the Hawaiian Ridge to the south. These small vents are distinct from the extensive regions of high backscatter occurring to the east that were interpreted to be young lava flows erupted through fissures near the crest of the Hawaiian flexural arch (Normark et al., 1988; Holmes et al., 1986, and Clague et al., 1989 and1990). The North Arch flow field, located north of Oahu, also includes hills of vesicular pillow basalt and hyaloclastite of alkalic basalt to nephelinite composition (Clague et al., 1990). These hills appear on the GLORIA images as small round spots of higher backscatter within the regions of high backscatter that represent the extensive flows. We have imaged a field of about 25 small high-backscatter volcanic mounds that appear similar to those in the North Arch flow field. We suspect that these mounds, located near 26°00'N, 163°20'W, are similar young vents of alkalic lava erupted through the Hawaiian flexural arch perhaps 10 Ma.

1d. Cretaceous ridges

Six small elongate ridges occur in the eastern part of the survey area (fig 5). These ridges are oriented at 254°-259° (avg. 257°), roughly parallel to the Murray Fracture Zone and perpendicular to the horst-graben lineations of the seafloor. These ridges are along the western edge of a region characterized by many small to large ridges with the same orientation (seen in the GLORIA images from cruise F6-88-HW). The ridges apparently formed along leaky transform faults or as coalesced seamounts formed at the spreading center. Analysis of rocks recovered by dredging on several of these subparallel ridges where they transect the North Arch lava flow field (Clague et al., 1989), demonstrates that these are old features unrelated to Hawaiian volcanism.

1e. The Hawaiian Arch Fault Zone

The Hawaiian Arch Fault Zone is a region on the arch north of the ridge that has about ten linear to sinuous faults (fig 5). The zone is about 150 km long and 30 km wide, and is centered near a large seamount located at 25°40'N, 164°20'W. The zone trends about 295° roughly parallel to the trend of the Hawaiian Ridge to the south. The fault scarps face the ridge (south) and down throw is also to the south. The faults vary in length from 10 to 100 km, and are characterized by crenulated or zig-zag offsets near their terminations. The longest fault is sinuous and has the zig-zag nature. It trends roughly 290°, and,

where it meets the large seamount centered in this zone, it skirts along and around the base of its southern flank.

These faults are interpreted to result from tensional fracturing of the crust along the crest of the arch; based on the near orthogonal crossing of the horst-graben structure and zig-zag nature of the faults, they are believed to postdate the formation of the horst and grabens that define the seafloor fabric created near the East Pacific Rise some 90 Ma. These faults may follow pre-existing weakness in the crust, thereby creating the zig-zag pattern, or the zig-zag nature may also result from reactivation of small sections of old fault planes along the horst-graben structure. Faults similar to these occur in the region to the east surveyed during cruise F6-88-HW. Although there are no voluminous flows along this portion of the Arch, we suspect that these types of faults may be pathways along which the voluminous North Arch lavas reached the surface (Holcomb et al., 1988, Normark et al., 1988, and Clague et al., 1989 and 1990).

1f. Magnetics

Total field magnetics were converted to give magnetic anomaly data by using the 1985 IGRF. Plots of magnetic anomaly along track showed the characteristic low-amplitude anomalies typical of ocean crust of this age. Despite this, several interesting features were noted. A small un-named seamount 135 km east of Necker Island produced the largest anomaly of the cruise, a +750nT positive anomaly. The seamount group around 25.6°N, 164.2°W showed anomalies ranging between +150 and -300nT. Chopin Seamount (fig 5), the flanks and center of which were surveyed on three lines, has very large magnetic anomalies associated with it. The line across the center of the seamount (line 28) records a negative anomaly of -700nT, wheras the lines immediately to the north and south of it show positive anomalies of +150nT and +400nT respectively. This large change in anomalies across the seamount is likely to result from variations in the types (and composition) of the intrusive and extrusive igneous rocks that form the seamount, or to magnetic field reversals. Owing to the 16 mile line spacing, this was the only seamount in our study area that we covered with more than a single trackline.

The anomalies along the flanks of the Hawaiian Ridge range from +500nT to -450nT. The large slides described later in this report are not apparent on the magnetic anomaly data, however, two large blocks from a rotational slump that is well imaged by GLORIA, are. These blocks (23.5°N,163.2°W;

23.7°N,163.2°W) are located immediately downslope from a magnetic anomaly high of +400nT. Each block (one on line 6, one on line 8) is associated with a prominant positive magnetic anomaly, +450nT for the block on line 6, and 200nT for the block on line 8. The ambient magnetic anomaly on either side of these blocks is +/- 100nT.

The Murray Fracture Zone lies in the northeast quadrant of our survey area (fig 3), and has prominant anomalies of -550nT across the southernmost of its transform valleys. Coverage of its northern transform valley is not adequate to describe in detail.

2. Sedimentation

2a. Sediments and 3.5 kHz echo character

Pelagic and volcanogenic sediments blanket the seafloor, and sediment thickness is a function of age of the crust, proximity to the Hawaiian Ridge, and transport directions and processes. Sediment mapped during this survey is typically thicker than that mapped by previous legs, reflecting the older age of the island chain in this region. 3.5 kHz echosounder penetration ranges from nearly zero over the higher peaks and ridges up to 45 m in the Hawaiian Trough that surrounds the ridge. Typically, areas with thicker sediment cover are characterized by very low backscatter areas on the sonar images, whereas areas with thinner sediment cover are characterized by higher backscatter.

Based on the two-channel seismic reflection profiles, sediment thickness ranges from a few meters to over 375 m (0.5 sec) in the deeper basins of the Hawaiian Trough. The thickest sediment is found in deep basins located in the Murray Fracture Zone, where up to 0.8 sec of sediment is profiled.

Bottom sediment and rock types are arranged into five groups based on 3.5 kHz echo character: (1) transparent sediment, (2) discontinuously stratified layer, (3) stratified-prolonged layer (4) opaque reflectors, and (5) hyperbolic reflectors. Figure 6 shows examples of the types of reflectors discussed in the following section.

The transparent layer (fig 6a, 6b, and 6d) is characterized by a moderate to strong bottom return, may have minor weak internal stratification, and ranges in thickness from less than a few meters on the ridges and distal parts of the arch, to over 25 m in the Hawaiian Trough. This layer typically thins away from the trough as one heads north onto the arch, and is only sporadically seen on

the seamount crests and slopes. This echo type is similar to one described by Torresan et al. (1989) draping the seafloor and overlying a discontinuously stratified unit. In places it grades laterally into a laminated or even stratified-prolonged or opaque echo type. The transparent layer is interpreted to be composed primarily of pelagic and some fine-grained volcanogenic sediment. The thicker nature of this unit along this portion of the Hawaiian Ridge reflects the increased age of the Hawaiian volcanoes, the lack of recent volcanic activity, and gravity-induced transport processes.

The discontinuously stratified unit is typically, but not always, overlain by the transparent drape (fig 6a, 6b, and 6c), although the drape can grade laterally into this laminated unit. It is typically discontinuous in its stratification, is characterized by weak to strong internal reflectors, and is more of a basin fill sequence. Unlike the transparent drape, this unit is interpreted to comprise the turbidite and other sediment gravity deposits associated with the more active phases of island growth and degradation. It commonly fills the lows between the debris blocks derived from the massive failures (both the slump and debris avalanche deposits) that characterize the Ridge flank and surrounding trough.

The stratified-prolonged layer is distinguished by a semi-prolonged to prolonged echo type with weak to discontinuous internal stratification (fig 6d and 6e). It is more common on the arch north of the trough. It is not as thick as the discontinuously stratified or transparent layers, and is either overlain by the transparent or discontinuously stratified layers (fig 6d), or is at the surface with no cover (fig 6e). This stratified-prolonged reflector is similar to that described by Wallin (1982). Where this reflector was cored, Wallin (1982) described a diverse range of compositions from a uniform brown clay to a coarse reworked semi-indurated volcaniclastic sand. Where this reflector is more prolonged, the sediment is a semi-indurated heterogenous mixture of silty clay beds, volcaniclastic sands, and ash layers with interspersed basalt fragments, glass, palagonite, and manganese crusts and nodules (Wallin, 1982).

The opaque reflector is an unusually strong and prolonged reflector that completely masks any subbottom (fig 6f). It is mainly associated with the steep and unfailed flanks and tops of the ridges and seamounts common throughout the region. This echo type is thought to indicate hard surfaces with little or no sediment cover.

The hyperbolic reflectors (fig 6g and 6h) have a variety of subtypes and can be subdivided mainly by size and elevation. They are indicative of irregular

and rough seafloor, caused by either gullied slopes, rough bedrock bottoms, or steep and irregular flanks of seamounts or ridges. However, most commonly the large and intense hyperbolic reflections are associated with the debris avalanche deposits that are widespread throughout the region. Many of these larger and intense hyperbolic reflections are covered by up to 45 m of transparent drape and discontinuously stratified sediment as measured from the 3.5 kHz profiles. The hyperbolic reflections represent jumbled blocks of debris derived from the massive failures that typify the flanks of the islands and adjacent seafloor.

2b. Sediment thickness and dispersal patterns

Sediment fill and distribution, based on 3.5 kHz penetration and two-channel airgun profiles, is complex. Sediment is thickest in the moat (Hawaiian Trough) adjacent to the Hawaiian Ridge, where it reaches up to 45 m on 3.5 kHz profiles, and over 0.5 sec on two-channel airgun records. The wedge generally thins to the north up on to the the arch, but further north past the crest of the arch, the total sediment package thickens again as the depth increases. The horst-graben complex is covered by varying amounts of sediment, with the lows (grabens) typically having thicker cover than the adjacent highs (horsts). Transparent sediment that overlies a laminated unit drapes the seafloor, and reaches thicknesses of up to 30 m. In many instances the transparent layer wedges out against the slopes of horsts or seamounts, and it is common for the sediment thickness on one side of a local high (horst, ridge, or seamount) to be radically different from that on the other side. The transparent layer grades laterally into laminated, prolonged, or stratified-prolonged reflectors, and a review of Wallin (1982) will give one a better understanding of the complexity of the sedimentation patterns on the arch.

A spectacular section is seen in the Murray Fracture Zone with the 3.5 kHz attaining 30 m of penetration, and the airgun profiles penetrating 0.8 sec into well-layered fill. It is unclear how such thick sediment has accumulated within and around the Murray Fracture Zone.

Based on the variety of sediment features seen on the GLORIA mosaic and geophysical records, an extensive review of mid- and north Pacific bottom circulation is required before determinations of sediment transport pathways and sources can be fully identified. The transparent drape varies both to the

north as well as to the east and west, and it appears that complex bottom currents control sedimentation in the region.

2c. Apparent Bedform Field

The Gloria mosaic shows a particularly interesting apparent bedform field whose apex is located on the ridge about 100 km east of Necker Island, at 23°30'N, 163°6.5'W (figs 7 and 8). This field appears to start at or near the same amphitheater that heads the northeast Necker Island debris avalanche (see following section on debris avalanches), and extends 110 km out onto the arch. The apparent field covers an area of about 1500 km^2, is conical in plan view, is about 5 to10 km wide near its apex, and over 30 km wide at its distal end (figs 7 and 8). The field terminates on its east side at a seamount with subdued backscatter, and it is flanked on its west by the northeast Necker Island debris avalanche.

The wavelength of the apparent bedforms is about 1.5 to 2 km on average, but varies from 0.5 to 3 km over the whole area. Based on detailed examination of the 3.5 kHz profiles over the area (fig 7a, 7b, and 9d), it is possible that this deposit is an older failure than those surrounding it, and consequently, has been covered by a thicker sediment cap owing to its increased age (Torresan et al., 1990). This thicker sediment cap masks the blocky character of the debris avalanche. The deposit could also result from continuing deposition of successive sediment gravity flows such as turbidites or debris flows. These apparent bedforms may be fed by the intricate network of gullies or submarine canyons that are incised into the ridge; such canyons characterize much of the upper portions of the Hawaiian volcanoes, especially in the amphitheater headwalls of the massive failures. A third hypothesis for the formation of the apparent bedforms is that they are an earthquake-triggered seris of slump folds, caused by partial mobilization and deformation of soft sediment. Other more subtle apparent bedforms occur in the survey area to the west and about the same distance from the Hawaiian Ridge, but they are too poorly defined to warrant a detailed description.

3. Island degradation: debris avalanches, slumps, and sediment gravity flows.

3a. Debris Avalanches

At least nine complete debris avalanches and portions of a few others were imaged during the survey. Although they are similar to the Hawaiian failures described previously (Lipman et al., 1988; Moore et al., 1989; Torresan et al., 1989; Normark et al., 1989; and MacGregor et al., 1989) they are generally smaller and more subdued by sedimentation owing to the greater age of this part of the Hawaiian Ridge. In some places more that one avalanche coalesced to form a larger deposit, much like the Nuuanu-Wailua complex located north of Oahu and Molokai (Moore et al., 1989).

Figures 5 and 8 show the locations and extent of all failures imaged during the F11-89-HW survey. The French Frigate Shoals debris avalanches are situated about 40 km northwest of Necker Island, extend for nearly 130 km along the Hawaiian ridge, and moved roughly due north off the ridge. The complex comprises two or maybe three different failures that travelled about 80 km from their headwall scarps, and cover an area of roughly 2500 km^2 for the combined complex. The deposit is similar to those described in the younger parts of the chain (Moore et al., 1989; Lipman et al.,1988; Normark et al., 1989; and Torresan et al., 1988). It is particularly similar to the Nuuanu-Wailau complex north of Oahu and Molokai, in that it is composed of more than one deposit. The field of blocks appears to be two deposits that actually cross paths; the more westerly of which travelled to the NE, and the more easterly and closest to Necker Island, which moved to the NW.

Apparent block size varies from a minimum of pixel dimensions (about 125 x 50 m) to a maximum of about 1 x 2 km. This contrasts with the younger deposits to the southeast that are commonly composed of a greater number of both smaller and larger blocks. Because the debris avalanche deposits along this part of the ridge are covered by thicker sediment (up to 45 m on 3.5 kHz profiles) the blocks must certainly be larger than what is exposed at the seafloor. This is true for all the debris avalanches and slump deposits imaged along this portion of the Hawaiian chain.

Most of the visible blocks for this deposit have travelled less than 60 km from their apparent headwall scarp, although some are up to 80 km away. Unfortunately, the thicker sediment cover not only makes the determination of

maximum block size impossible, it also masks the actual termination of this complex, which probably is somewhere higher on the arch than is detectable from the GLORIA mosaic and the seismic profiles. The northeast Necker debris avalanche heads out from a point 90 km southeast of Necker Island, and is associated with an amphitheater-shaped scallop on the ridge located at about 23°25.0'N, 163°35.0'W. It travelled about 80 km from its headwall scarp on the ridge, and varies from about 5 km wide at its apex to 15 km wide at its termination on the distal end. The failure is a relatively narrow feature unlike the more lobe-shaped debris avalanches that characterize the ridge, and trends about 345°, having moved in a northwesterly direction from its source. The avalanche deposit covers an area of about 950 km^2, and it is fed at is source by a smaller debris avalanche that covers an area of about 300 km^2. The distal portion of the northeast Necker deposit is flanked by Necker Island on its west and a large apparent bedform field (perhaps a buried failure; see preceeding section) on its east. Block size for the combined deposits varies from about pixel dimensions to blocks about 1 x 2 km on a side, and, like the previously described deposit, much of it is covered by relatively thick transparent and discontinously-stratified soft sediments. On 3.5 kHz profiles (fig 9), buried blocks appear as chaotic and hyperbolic returns that are draped by transparent sediment, in contrast to the younger debris avalanche deposits further east along the chain (Lipman et al., 1988; Moore et al., 1989; and Torresan et al., 1990).

Unnamed debris avalanche deposits occur between the Nihoa Island and Necker Island debris avalanche deposits on its east and west respectively (figs 5 and 8). Like the deposits described above, the complex comprises two failures, a smaller one to the east that feeds into a larger, more lobate failure on the west. The smaller of the two failures heads from a location about 23°20'N, 162°45'W into the larger failure, and the larger heads from an amphitheater located about 23°25'N, 162°50'W. Together they moved slightly east of north for 110 km across the trough and onto the arch. The failures cover areas of about 250 km^2 and 4400 km^2; the smaller failure measuring 25 x 10 km, and the larger measuring about 110 x 40 km. As is typical for the failures along this portion of the ridge, both are draped by a relatively thick sediment cover, and apparent block size varies from pixel dimensions to a maximum of about 1 x 2 km on a side.

Our survey also covered the distal portions of the Nihoa Island debris avalanche deposits that have reduced Nihoa Island to a small vestige of its

former self as it has been eroded by massive failures from all sides. A detailed description will not be given here except to say that the failures are larger than those imaged during our survey. More detailed information is available in MacGregor et al. (1989) and in data collected on the F6-88-HW GLORIA survey.

1b. Slumps

The St. Rogatien Bank slump is located about 200 km west of Necker Island along the Hawaiian Ridge. Figures 5, 8, and 10 are traced from the GLORIA mosaic, and show the major features comprising this failure. The slump mass extends nearly 180 km along the ridge, from 24°15 N, 166°25W to 26°40N, 167°25W, and forms a broad arc that has significantly modified this portion of the ridge (figs 5, 8, and 10). The slump is similar to the Waianae slump described by Hussong et al. (1987), Torresan et al. (1989), and Moore et al. (1989).

The slump extends 30 to 35 km from the shoal portion of the ridge, and covers an area about 6000 km^2. On line 8, the slump is seen to be divided into 5 major rotational blocks from 2 km to 5 km in width, and are surficially expressed as transverse ridges with back-rotated surfaces (figs 10 and 11). These back-tilted surfaces face the ridge, forming basins from 15 to 115 m in depth filled with 5 to 35 m of sediment in their deepest parts.

Our interpretation was aided by three transects normal to the ridge (lines 6, 8, and 10) and therefore through the different segments of the arcuate-slump. The four large ridges range in length from about 10 km to 100 km, are spaced from 2 to 6 km apart along line 8, the central transect (fig 11), and rise from 15 to 115 m above the adjacent slope. The blocks have scarps that vary from about 100 to 540 m above the adjacent down-thrown block, and have slopes in the 20 to 25° range. The uppermost block is about 2950 m below the crest of the bank (fig 11), and has about a 25° slope. Overall, the slump has an elevation change of 4350 m over the 37 km from the seafloor at the base of the ridge to the crest of the bank (from 800 m to 5150 m; fig 11). In contrast, average slopes for the underwater flanks of the ridge are about 9°. Similar to the Waianae slump, the steep toe, large width:length ratio, and general lack of a hummocky surface indicates that it moved as a few large blocks rather than as a debris avalanche.

Two other crossings (lines 6 and 10) show similar features except that the slump is broken differently across these transects as evident from the GLORIA images and profiles taken across these lines. Line 6 defines possibly

seven back-rotated blocks all situated below steep scarps that range from a minimum of 20 m to a maximum of about 2750 m. The transect across line 6 is marked by a steep slump toe that rises over 1300 m across 8 km, from the basin turbidites over 5000 m deep, to an enclosed trough (formed by a back rotated block) at about 3800 m depth. Line 6 also shows another impressive scarp of 2745 m between two major blocks, located between depths of 940 m and 3790 m. The back-tilted blocks define perched basins that vary in depth from a minimum of 20 to over 300 m and contain ponded sediment with up to 35 m of chaotic and stratified fill.

Line 10, although not as long nor starting as shallow as lines 6 and 8, shows much the same morphology and slump associations. Here the slump mass defines about 6 back-rotated blocks, a steep toe of about 700 m rising from the basin at 5100 m deep, and a headwall scarp of over 1000 m. Similar to the other profiles, back-rotated surfaces below steep scarps define ponded basins ranging from about 20 m to over 100 m in depth, and having 5 to 15 m of fill.

In addition to the major blocks that compose this slump, the northern termination of St. Rogatien Bank (north of line 10) has broken into a debris avalanche-style failure, where slump blocks have detached from the main mass and travelled out into the trough, both to the north and southeast, up to 40 km away from the ridge (figs 5, 8, and 10). Block size at the northern termination varies from 2 x 12 km to 0.5 x 1 km. We infer that the slumping along this termination was accompanied by a subsequent debris avalanche.

The two styles of submarine failures observed along this part of the ridge (slumps and debris avalanches) are identical to those imaged by all previous Hawaiian GLORIA surveys, except that they have more sediment cover than the younger slides (fig 9). There is likely a broader spectrum of failure styles associated with these failures, but recognizing them and fully understanding their mechanics and their association with island growth and evolution requires more detailed observations, sampling, and analysis of both old and young failures.

Like the associations discussed by Moore et al. (1989), a slump is steeper, thicker, and wide relative to its length when compared to debris avalanche failures. The St. Rogatien Bank slump has a steeper gradient than the avalanches, and the width/length ratio exceeds one. Unlike the avalanches, the slump has maintained its physical continuity, not moving far from its source and not breaking into smaller debris blocks that litter the seafloor. The implica-

tion is that the slump moved slowly and at low velocities. The slump is marked by steep scarps at both the head and toe, back-rotated blocks, and transverse ridges and scarps that are bounded by faults.

The debris avalanches described above are also associated with distinct amphitheaters at their heads that likely mark the source area from which the avalanche material was derived. Blocks travel out beyond the moat and onto the arch, but unlike the younger failures to the southeast, true block size and actual runout distance is masked by the thicker sediment cover (up to 45 m of transparent and discontinuously stratified material based on 3.5 kHz penetration; fig 9). The distal portions of the debris avalanche deposits probably is gradational into turbidity flows, although the actual deposit associated with a single event is not discernable from the data.

The failures are probably associated with and modify volcano development. Steep unbuttressed slopes and the hydraulic jacking associated with dike and magma injection into dikes along rift zones are the most likely causes, and the failures are more prone to occur during the vigorous phases of volcanic activity and island growth. In the case of these volcanoes, the active growth phase was about 7-13 Ma.

3c. Sediment gravity deposit off northern Necker Island

A probable sediment gravity deposit was imaged on the northeast side of Necker Island. Its presence is evident on the GLORIA mosaic as a zone of slightly higher backscatter that defines a channelized (?) linear deposit that has a lobate termination (fig 8). The flow heads nearly due north from a position on the upper flank of the Necker ediface located at 23°50'N, 164°25.0'W, and is 65 to 75 km long.

An interesting observation about the distal part of the deposit is that it appears to be neatly split by a flat topped seamount located 75 km from its origin on the island flank. The GLORIA mosaic shows an apparent splitting of the flow around the ediface much like the appearence of a boulder in a stream or bow wave, where the flow separates and skirts around the obstacle. The south side of the seamount is characterized by an apparent moat that may result from scouring at its base by the rapidly moving deposit.

3d. Small-scale mass wasting - ridge crest and flank gullying

The top of the ridge along the chain is characterized by gullies or canyons possibly carved during lower stands of sea level, that are now conduits for smaller scale mass wasting and are herein termed debris chutes. Figure 12a, taken from a 3.5 kHz profile along line 5 and above the headwall of the St. Rogatien Bank Slump, details the cut and fill nature of these chutes. Figure 12b shows that the chutes are characterized by high backscatter and have a dendritic pattern. They either coalesce down slope forming one main conduit, or spread apart downslope, forming a birdsfoot pattern. They occur throughout the GLORIA surveys along the Hawaiian Ridge, and are likely important conduits for the movement of coarser debris downslope and into the surrounding deep. Their lower extremities may be carved and maintained by sediment gravity flows triggered by wave loading in shallower water or oversteepening of nearshore deposits, as they build through time.

4. Submerged carbonate reefs

Three bands of high backscatter were imaged on the north rift zone of Necker Island (figs 5 and 8). A single band of high backscatter occurs along the north rift zone of St. Rogatien Bank. All these high-backscatter bands occur near 1500 m water depth. These bands are similar in appearance to those imaged on the Kohala Terrace (Moore and Clague, 1988), the Haleakala rift zone (Moore et al., 1990), offshore of the Kona coast of Hawaii (Moore and Clague, 1987), off the east coast of the subaerial tip of the Mauna Loa southwest rift zone (Moore et al., 1990), and to the south of the island of Lanai (imaged on cruise F5-86-HW). In each case, further work, including dredging or submersible operations, has confirmed that these subparallel bands of high backscatter are drowned coral reefs. A reconstruction of sea surface isotherms through the Tertiary (Clague and Dalrymple, 1987, modified from Greene et al., 1978) shows that the surface water temperatures were marginal for growth of corals from about 5-15 Ma and too cold from 15-40 Ma at the latitude of Hawaii. The bands of bright backscatter on the north rift zone of Necker Island may be bryozoan-algal reefs, which tolerate cooler temperatures, rather than coral reefs (Schlanger and Konishi, 1975).

ACKNOWLEDGEMENTS

REFERENCES CITED

Batiza, R., 1989, Seamounts and seamount chains of the eastern Pacific, in: Winterer, E.I., Hussong, D.M., and Decker, R.W., eds., The Eastern Pacific Ocean and Hawaii: Boulder, Colorado, Geological Society of America, The Geology of North America, v. N, p. 289-306.

Chase, T.E., Menard, H.W., and Mammerickx, J., 1972, Bathymetry of the North Pacific: Scripps Institute of Oceanography and Institute of Marine Recources, chart no. 8.

Clague, D.A., and Dalrymple, G.B., 1987, The Hawaiian-Emperor volcanic chain, Part I: U.S, Geological Survey Professional Paper, 1350, Chapter 1, p. 5-54.

Clague, D.A., Moore, J.G., Torresan, M.E., Holcomb, R.T., and Lipman, P.W., 1988, Shipboard report for Hawaii Gloria ground-truth cruise F2-88-HW, 25 February - 9 March, 1988: U.S. Geological Survey Open-File Report 88-292, 54p.

Clague, D.A., Holcomb, R.T., Torresan, M.E., and Ross, S., 1989, Shipboard report for Hawaii GLORIA ground-truth criuse F11-88-HW, 25 Oct - 7 Nov, 1988: U.S. Geological Survey Open-File Report 89-109, 33 p.

Clague, D.A., Holcomb, R.T., Sinton, J.M., Detrick, R.S., and Torresan, M.E., 1990, Pliocene and Pliestocene alkalic flood basalts on the seafloor north of the Hawaiian Islands: Earth and Planetary Science Letters, v. 98, p. 175-191.

Dalrymple, G.B., Lanphere, M.A., and Jackson, E.D.,1974, Contributions to the petrography and geochronology of volcanic rocks from the leeward Hawaiian Islands: Geological Society of America Bulletin, v. 85, p. 727-738.

Fornari, D.J., Ryan, W.B.F., and Fox, P.J.,1984, The evolution of craters and calderas on young seamounts: Insights from SEA MARC 1 and Sea Beam sonar surveys of a small seamount group near the axis of the East Pacific Rise at ~ 10°N: Journal of Geophysical Research, v. 89, n. B13, p. 11069-11083.

Greene, H.G., Dalrymple, G.B., and Clague, D.A.,1978, Evidence for northward movement of the Emperor Seamounts: Geology, v. 6, p. 70-74.

Holcomb, R.T., Holmes, M.L., Denlinger, R.P., Searle, R.C., and Normark, W.R., 1988, Submarine Hawaiian North Arch volcanic Field: EOS, v. 69, p. 1445.

Holmes, M.L., Moore, J.G., Holcomb, R.T., and Belderson, B., 1986, Cruise report, Farnella F5-86-HW, windward Hawaii: U.S. Geological Survey, Branch of Pacific Marine Geology Administrative Report, 28p.

Lipman, P.W., Normark, W.R., Moore, J.G., Wilson, J.B., and Gutmacher, C.E., 1988, The giant submarine Alika debris slide, Mauna Loa, Hawaii: Journal of Geophysical Research, v. 93, p. 4279-4299.

Malahoff, A., and Woollard, G.P., 1968, Geophysical studies of the Hawaiian Ridge and the Murray Fracture Zone: in The Sea, v. 4, 1970, Arthur E. Maxwell ed., p. 73-131.

MacGregor, B., Kappel, E., and Wilson, J.B., 1989, Cruise report, Hawaii GLORIA cruise F10-88-HW: U.S. Geological Survey, Branch of Pacific Marine Geology, Administrative Report, _p.

Moore, J.G., and Clague, D.A., 1987, Coastal lava flows from Mauna Loa and Hualalai volcanoes, Kona, Hawaii: Bulletin of Volcanology, v. 49, p. 752-764.

Moore, J.G., and Clague, D.A., 1988, Offshore geology of Mahukona, Kohala, Mauna Kea, Hualalai, and Mauna Loa volcanoes to the northwest of Hawaii: EOS, v. 69, n. 44, p. 1445.

Moore, J.G., Clague, D.A., Holcomb, R.T., Lipman, P.W., Normark, W.R., and Torresan, M.E.,1989, Prodigious submarine landslides on the Hawaiian Ridge: Journal of Geophysical Research, v. 12, n. B12, p. 17465-17484.

Moore, J.G., Clague, D.A., Ludwig, K.R., and Mark, R.K.,1990, Subsidence and volcanism of the Haleakala Ridge, Hawaii: Journal of Volcanology and Geothermal Research, v. 42, p. 273-284.

Normark, W.R., Lipman, P.W., Wilson, J.B., Jacobs, C.L., Johnson, D.P., and Gutmacher, C.E., 1987, Preliminary cruise report, Hawaii GLORIA leg 2, F6-86-HW, November 1986: U.S. Geological Survey Open-File Report 87-298, 42p.

Normark, W.R., Holcomb, R.T., Searle, R.C., and Somers, M.L., 1989, Cruise report, Hawaiian GLORIA legs 3 and 4, F3-88-HW and F4-88-HW: U.S. Geological Survey Open-File Report 89-213, 56p.

Schlanger, S.O., and Konishi, K., 1975, The geographic boundary between the coral-algal and the bryozoan-algal limestone facies: A paleolatitude indicator: IX International Geological Congress of Sedimentology, Niece, Theme 1, Sedimentologic Indicators, p. 187-190.

Torresan, M.E., Shor, A.N., Wilson, J.B., and Campbell, J., 1989, Cruise report, Hawaiian GLORIA leg 5, F5-88-HW: U.S. Geological Survey Open-File Report 89-198, 55p.

Torresan, M.E., Clague, D.A., and Jacobs, C.L., 1990, Maturation of large scale masswasting along the Hawaiian Ridge: AAPG v. 74, n. 6, p. 1005.

Wallin, B.H., 1982, The northern Hawaiian Deep and Arch: Interpretation of geologic history from reflection profiling and echo character mapping: MS Thesis, University of Hawaii, Honolulu, Hawaii, 133p.

FIGURE CAPTIONS

Figure 1. Geographic location map of the entire Hawaiian Ridge showing
major landslides mapped as of the spring of 1990 with GLORIA. F12-89-
HW cruise area delimitted in dashed box. Slides around the main
islands are shown with dotted lines. Slides to the northwest are shown
with dashed lines because the position is approximate and based on
unprocessed data. Mapping of the Hawaiian Ridge west of 170° W is
incomplete; thus the distribution of deposits is poorly known, especially
on the north side of the Ridge. Contours are the 2000 and 4000 m
isobaths, and are adapted from U. S. Naval Oceanographic Office,
bathymetric atlas of the North Pacific Ocean (1973).

Figure 2. Trackline chart for F12-89-HW (Mercator Projection).

Figure 3. Tectonic elements of the Murray Fracture Zone; (a) GLORIA
Image; (b) Tracing from GLORIA mosaic showing major lineations of the
Murray Fracture Zone and lineations associated with the seafloor
spreading fabric.

Figure 4. Seafloor spreading fabric lineations (horst and graben) from a
portion of line 26; (a) GLORIA image; (b) 3.5 kHzprofile. High
backscatter lineations are the elevated ridges of the horsts. The lower
backscatter areas are the more deeply covered grabens.

Figure 5. Generalized map of the region imaged on F12-89-HW showing the
distribution of the variety of seamounts and ridges, the limits of mass
wasting features, submerged reefs, the Hawaiian Arch fault zone, the
Murray Fracture Zone, and the trend of the seafloor spreading fabric.
Explanation on following page.

Figure 6. 3.5 kHz seismic reflection profiles showing the 5 types of 3.5kHz
returns that characterized the study area. (a) Two transparent layers,
separated by a thin discontinuous layer, draping failed blocks of a debris
avalanche located along line 6. (b) Transparent layer over a discon-
tinous to continuously stratified layer along line 8. (c) Continuous to

discontinously stratified layer located along line 1. (d) Transparent layer overlying a stratified-prolonged reflector along line 18. (e) Stratified-prolonged reflector located along line 18 on the Hawaiian Arch. (f) Opaque reflector along line 4A from along the Hawaiian Ridge. (g) Hyperbolic reflectors along line 1. The hyperbolics result from the steep and rugged flanks of the Ridge that are incised by canyons and gullies. (h) Hyperbolic reflectors from both burried and exposed blocky debris that litters the seafloor adjacent to the Ridge (Line11).

Figure 7. (a) GLORIA mosaic constructed from images collected along lines 8 and 10, showing an apparent bedform field (the high backscatter ripple pattern in center of image), which is interpretted to be an older failure, with a thicker sediment cover than the (younger?) failures surrounding it. (b) 3.5 kHz profile along line 10, showing sediment draping debris blocks. Buried blocks are inferred from the diffractions and hyperbolics visible below the sediment drape. (c) 3.5 kHz profile along line 6, showing sediment cover (two separate tranparent layers separated by a thin discontinuous horizon) over failed blocks of a debris avalanche.

Figure 8. Map showing the extent of slide deposits and failure types (slumps and debris avalanches, and a possible sediment gravity flow) imaged on the north side of the Hawaiian Ridge between Nihoa Island and St. Rogatien Bank during F12-89-HW.

Figure 9. 3.5 kHz profiles across debris avalanche deposits. (a) Profile along line 6 on the lower flank of the Hawaiian Ridge. Note the hummocky topography and hyperbolic nature of some of the returns. Many of the debris blocks are capped by sediment, which has started to subdue the rugged nature of the deposit. Unlike younger failures around the principal Hawaiian islands the deposits along the older portions of the Ridge are charaterized by a subdued topography owing to a thicker sediment cover. (b) Profile across the northeast Necker Island debris avalanche (line 6) showing debris blocks draped with sediment. (c) 3.5 kHz profile along line 8 across a portion of the terminus of the French Frigate Shoals debris avalanche. This profile is farther away from the Ridge than are the preceeding profiles. Note how the blocks are draped

by a transparent layer that overlies a laminated, discontinuous to prolonged stratified layer immediately above the blocks. The blocky debris along this profile is subdued by subsequent sedimentation. (d) 3.5 kHz profile along line 8 showing blocky debris subdued by subsequent sedimentation.

Figure 10. Map of the St. Rogatien Bank Slump traced from the GLORIA mosaic. This slump like most others imaged around the Hawaiian Ridge is situated on a rift zone.

Figure 11. Seismic reflection profiles from the St. Rogatien Bank slump (Line 8). These profiles show that this feature is a rotational slump whose blocks have not travelled far (up to 35 km) from the source; (a) 10 kHz profile; (b) 3.5 kHz profile, note the back-rotated blocks and ponded sediment on the back-tilted surfaces of the failed blocks; (c) unprocessed two channel air gun profile.

Figure 12. Canyons and gullies incised into the upper flanks of the Hawaiian Ridge collected along line 5; (a) GLORIA image; note the high backscatter in central portion of image; (b) 3.5 kHz seismic reflection profile; note the rugged topography owing to the incised canyons and gullies characteristic of most of the upper flanks of the Ridge.
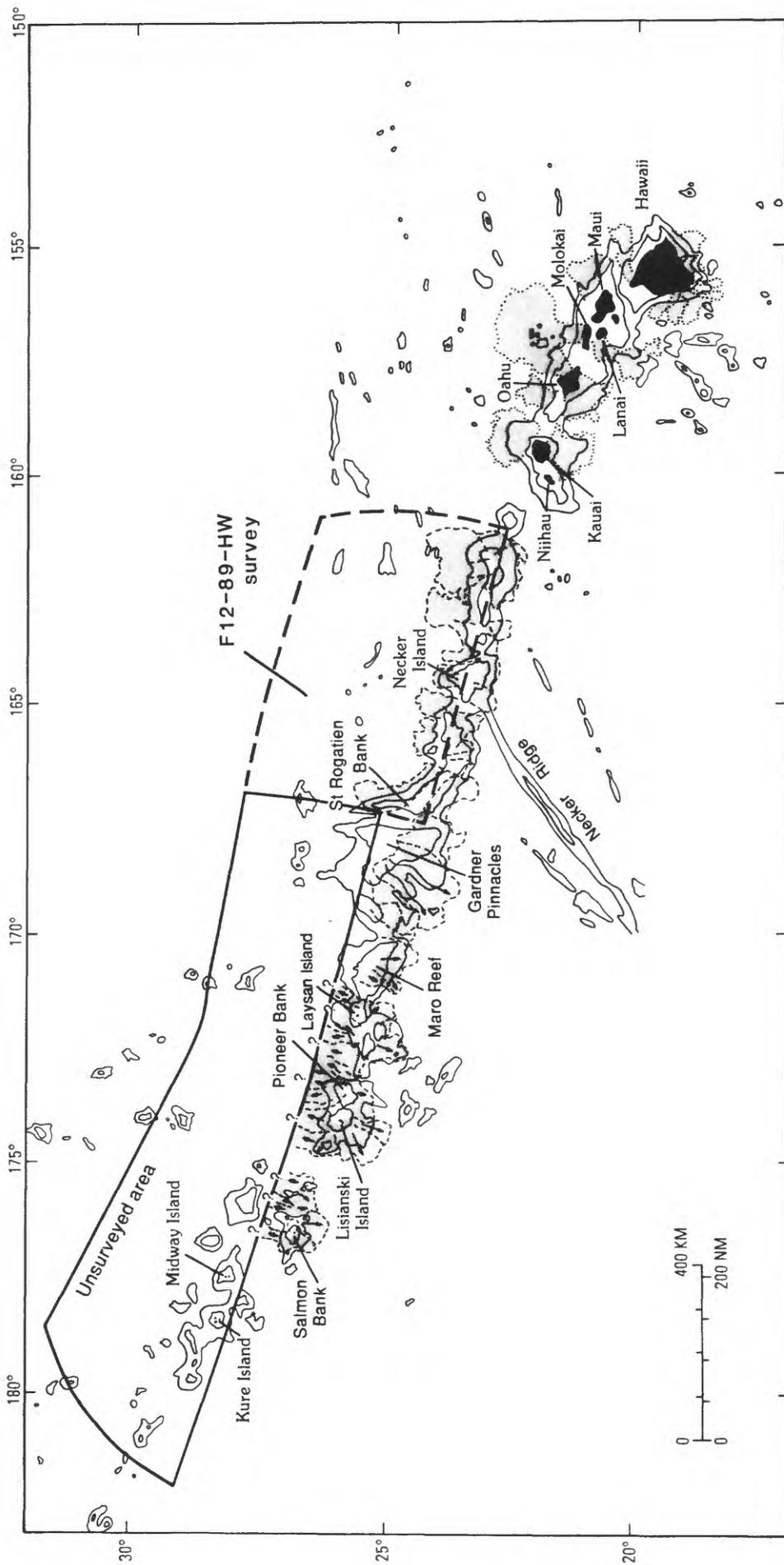
Figure 1
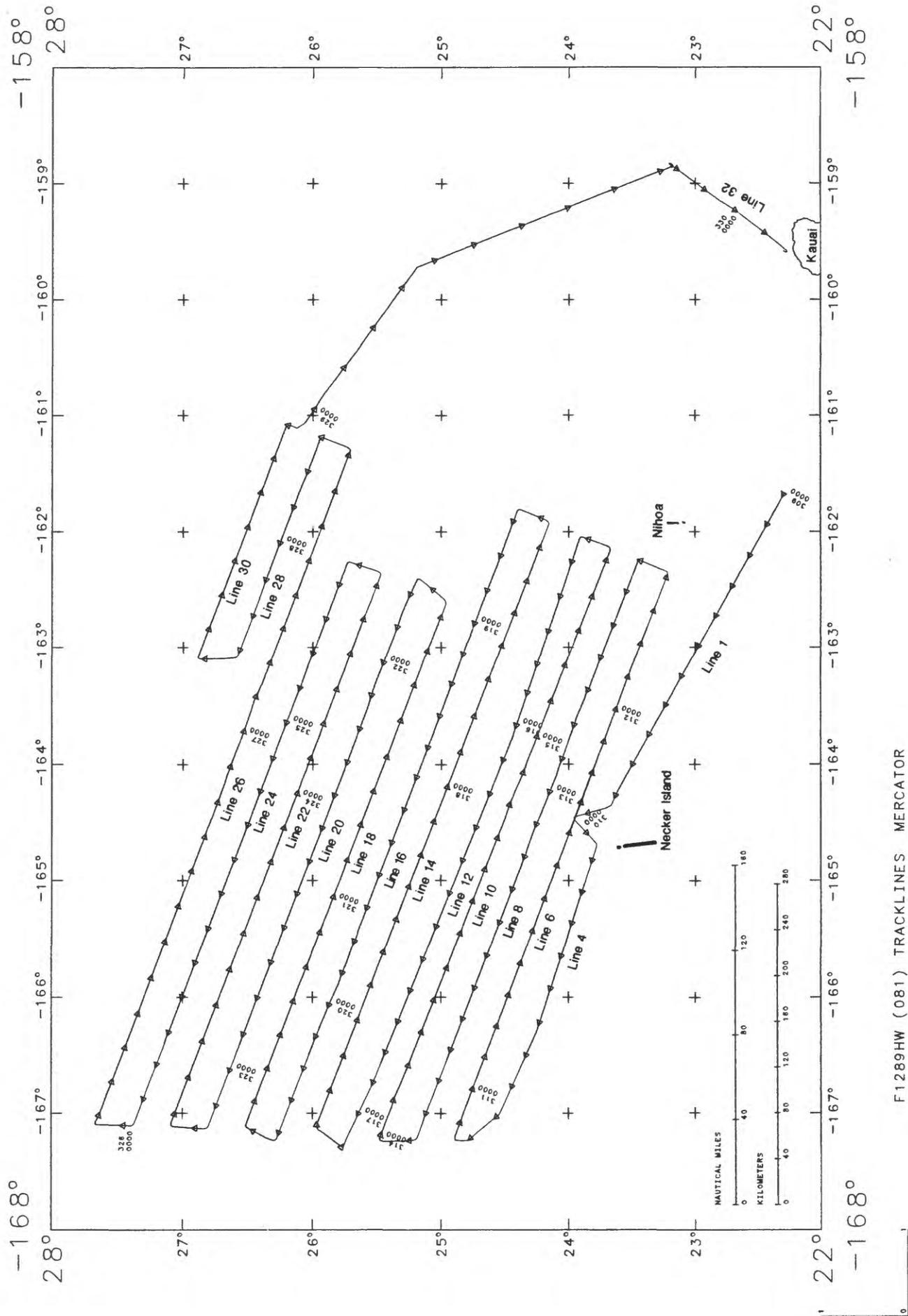
F1289HW (081) TRACKLINES MERCATOR

Figure 2

34
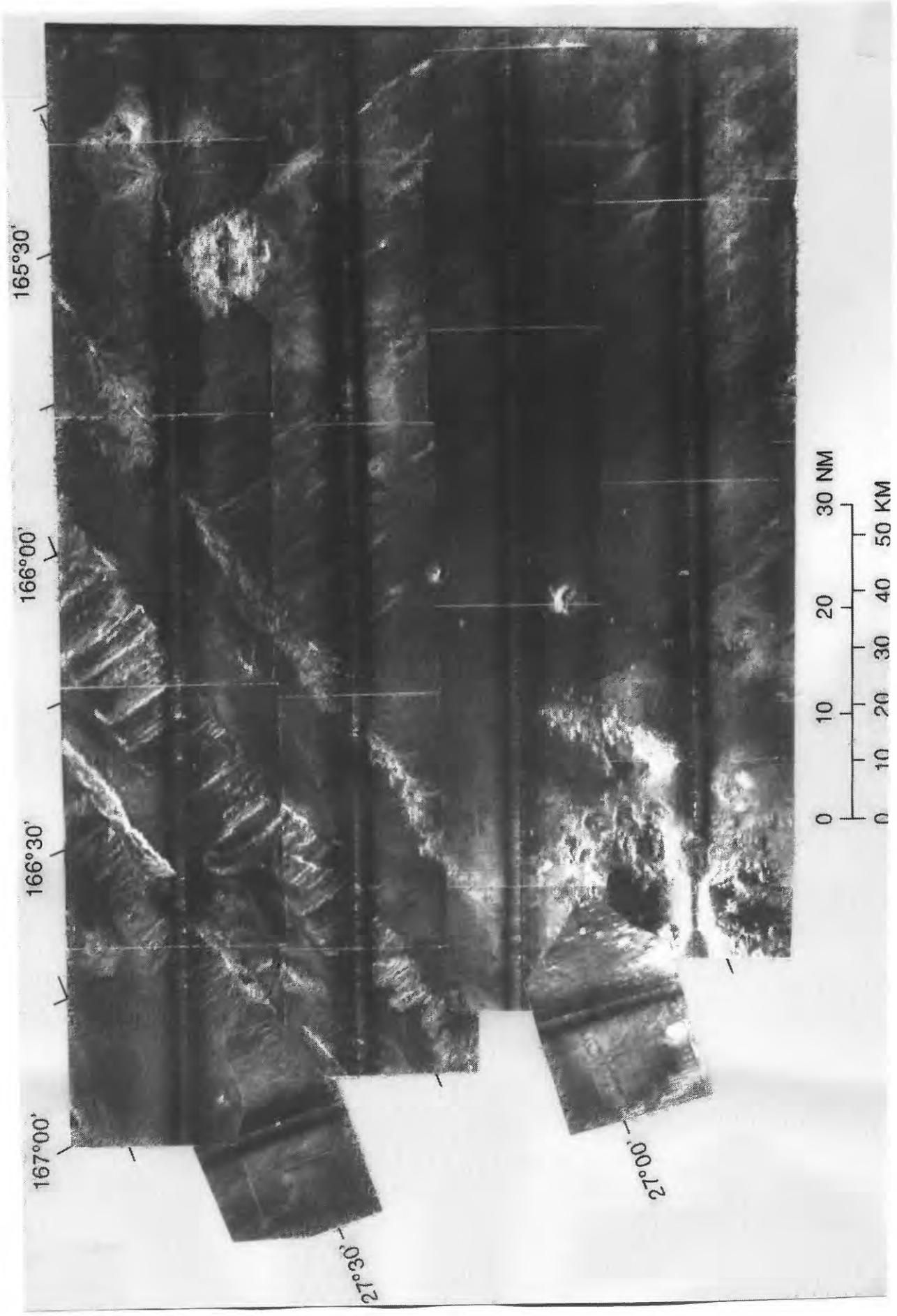
Figure 3a
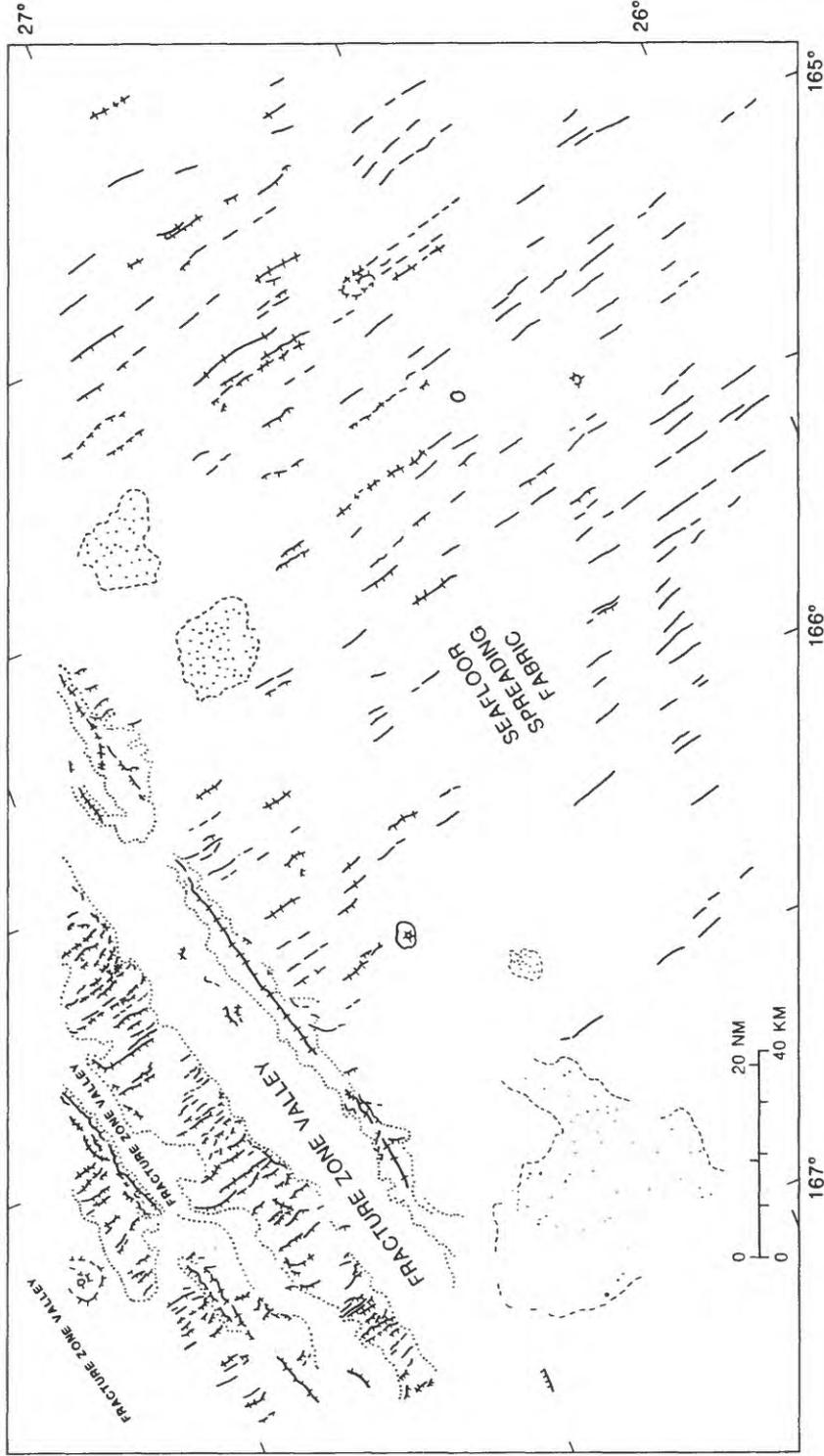
Small, fresh and
flat-topped
appearing seamounts

Old, eroded appearing
seamounts

Approximate trend
of ridge crest

Lineation of (scarp or ridge)
Murray Fracture Zone and
seafloor spreading fabric.
Hachures on down side

Trend of ridges/scarp of
the Murray Fracture Zone

Approximate base/boundary
of major ridge of Murray
Fracture Zone

Figure 3b

SEAFLOOR SPREADING FABRIC

Line 26 →

JD/GMT 326/1300 326/1400 326/1500 326/1600 326/1700 327/1800 327/1900

0   10   20   30 KM

0   5   10   15 NM
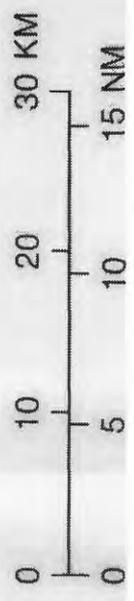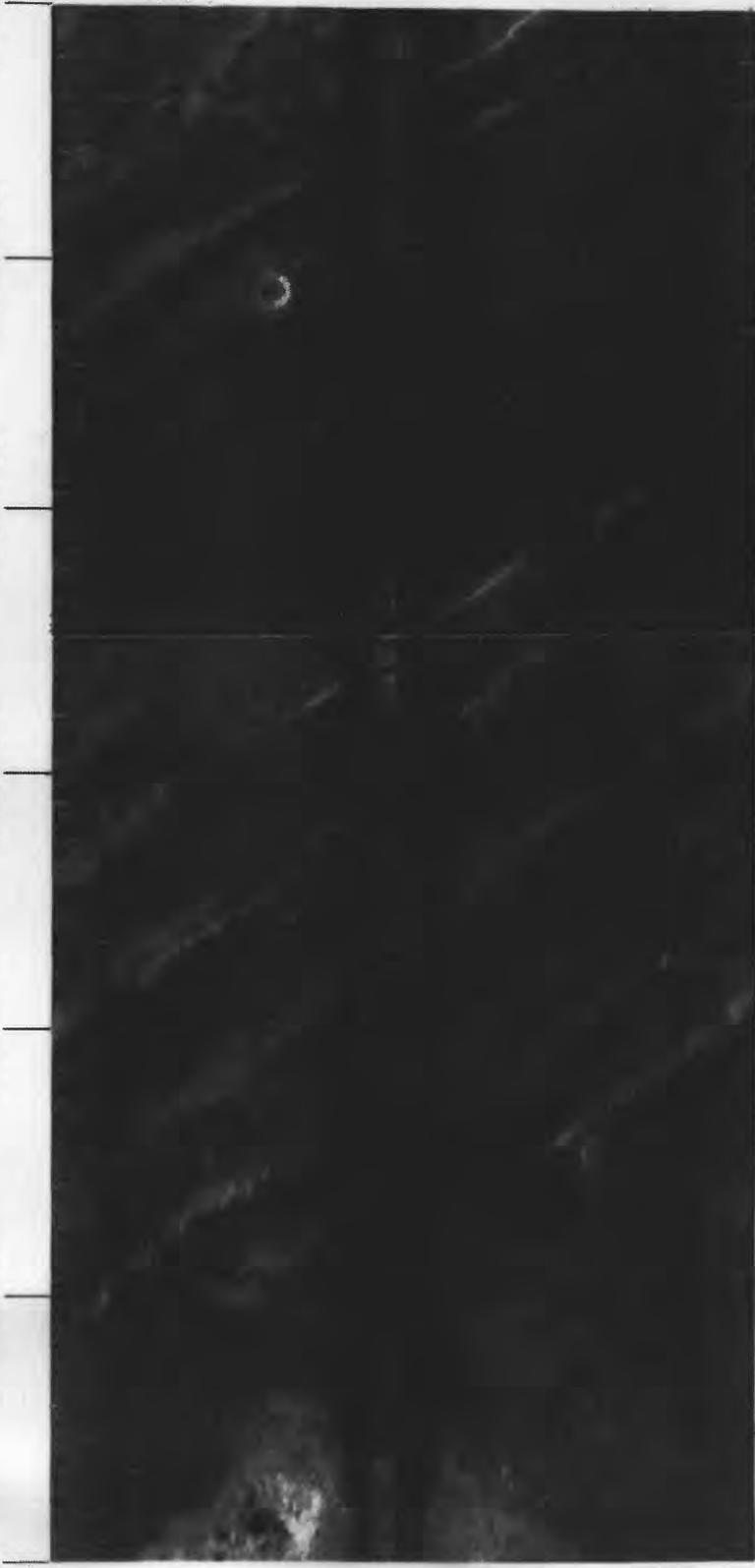
Figure 4a

Figure 4b

38
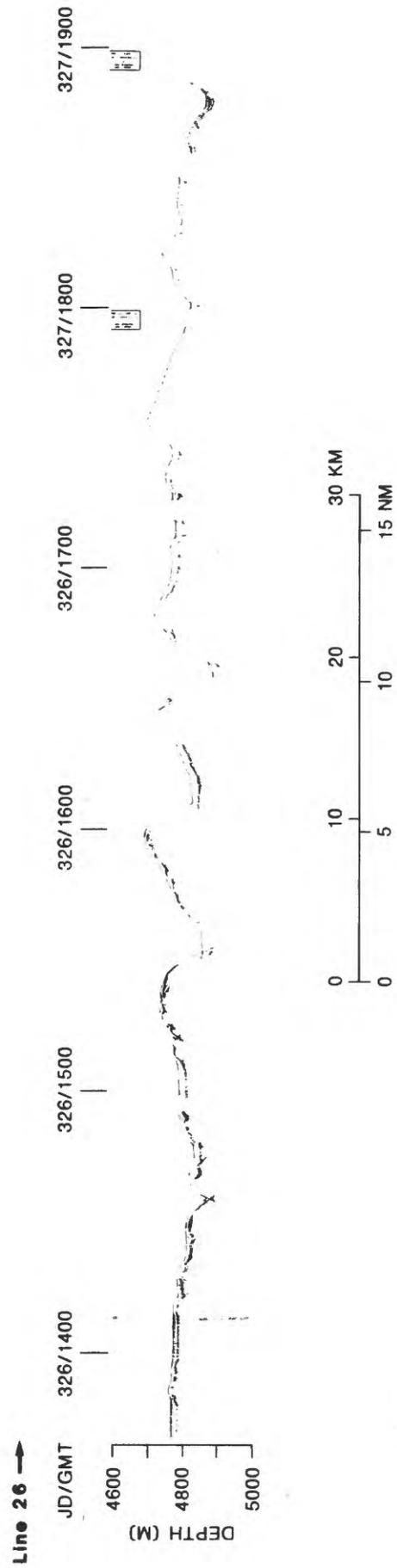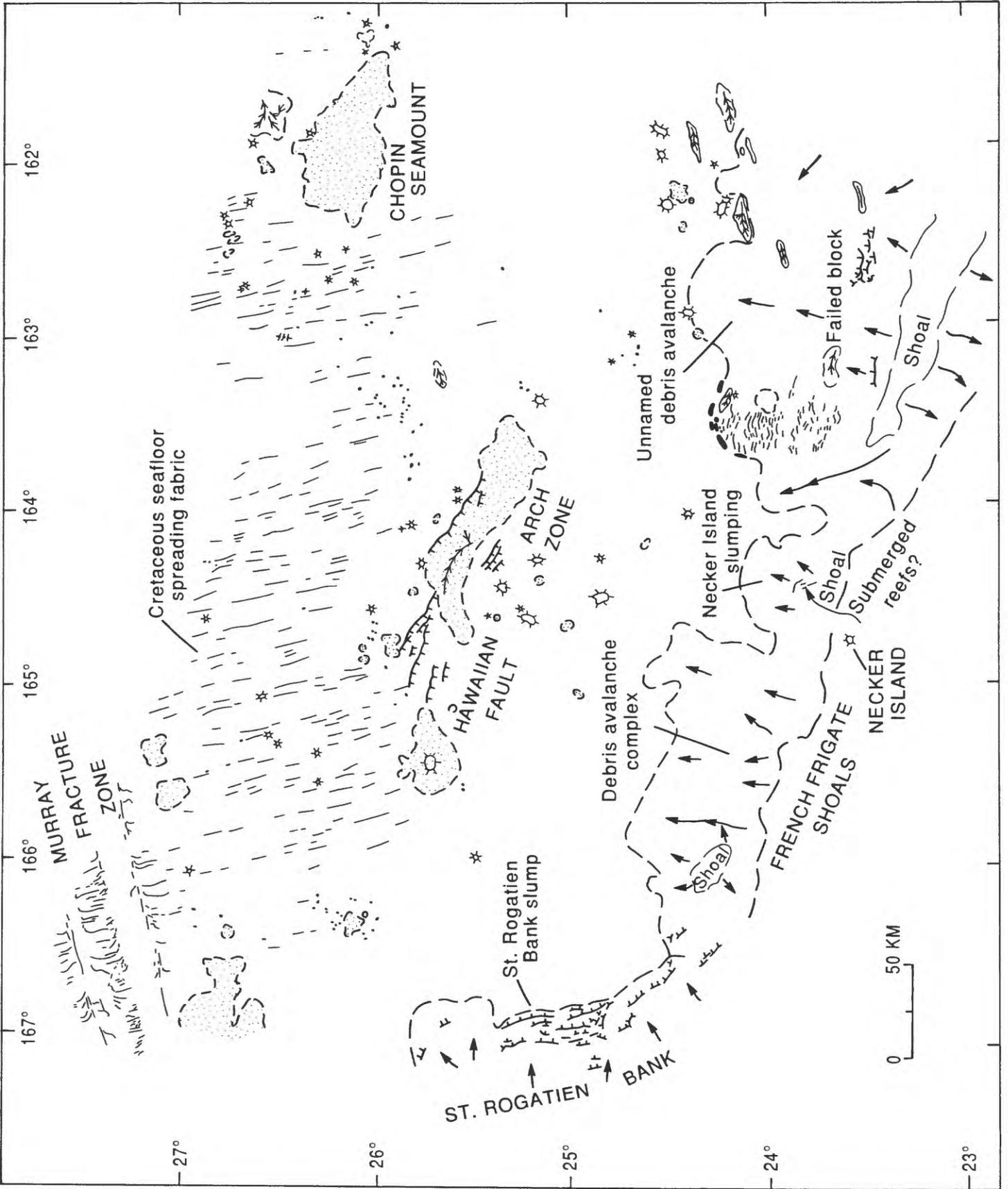
Figure 5

EXPLANATION

Scarp, hachures on downthrown side

Large flat-topped seamounts, part of Hawaiian Ridge

Small circular, low relief flat-topped seamounts; with or without summit caldera

Very small, high backscatter, rounded volcanic mounds located near the axis of the Hawaiian Arch

Cretaceous ridge

Seafloor spreading fabric

Approximate boundary of mass wasting (large failures)

Rough surfaced non-circular seamounts

Figure 6a

JD/GMT 313/0136   313/0148   313/0200   313/0212   313/0224   313/0236

WATER DEPTH, IN METERS

4500

4575   **LINE 8**   0   5 KM

4650

4725

4800

4875
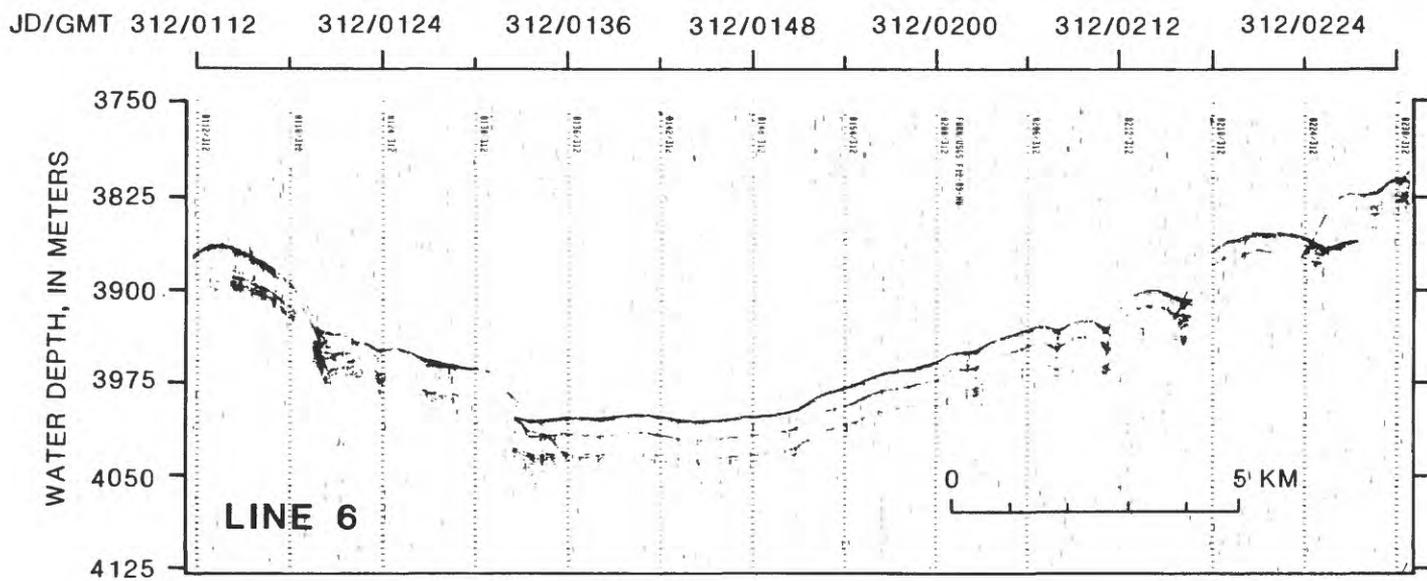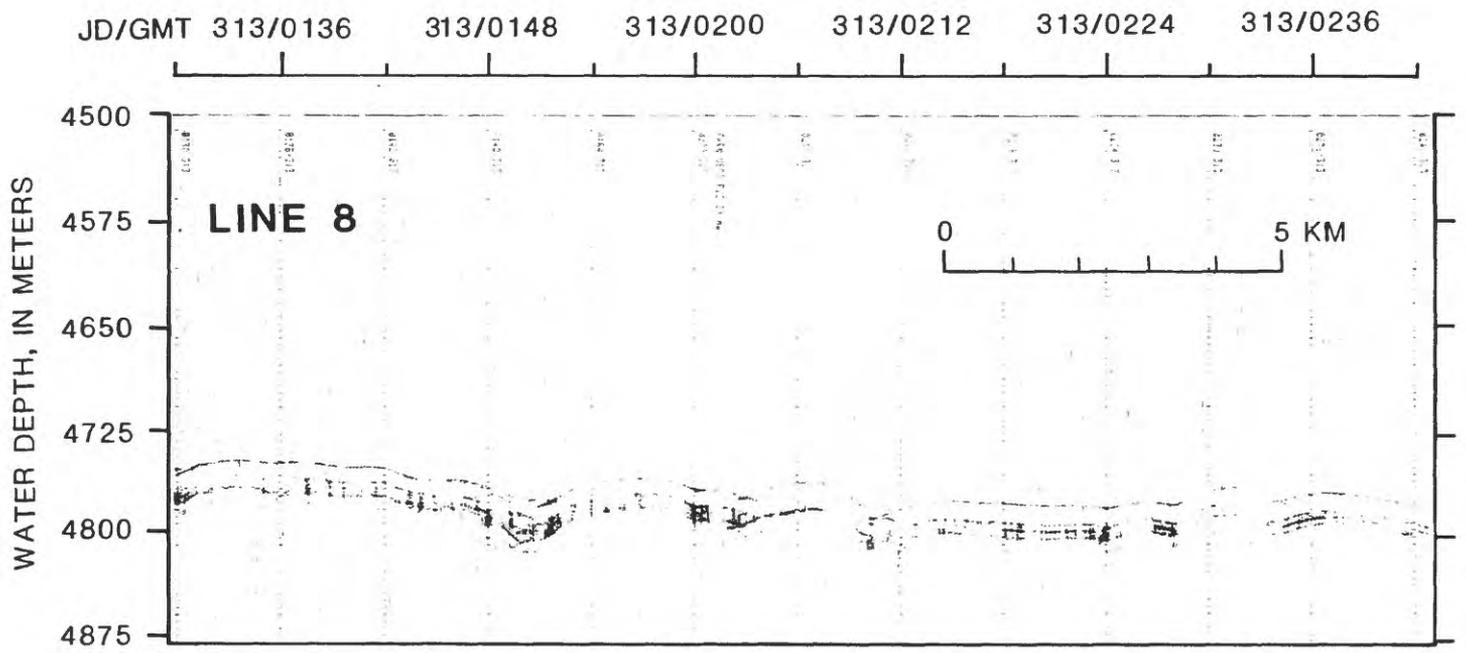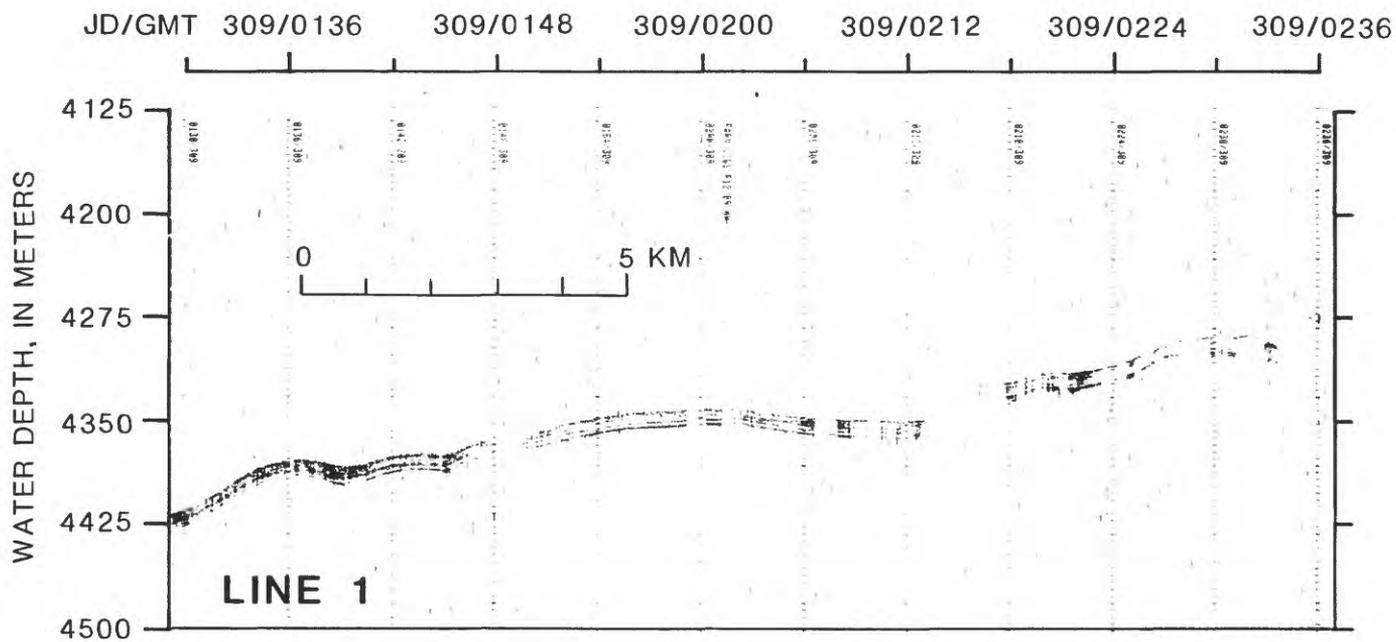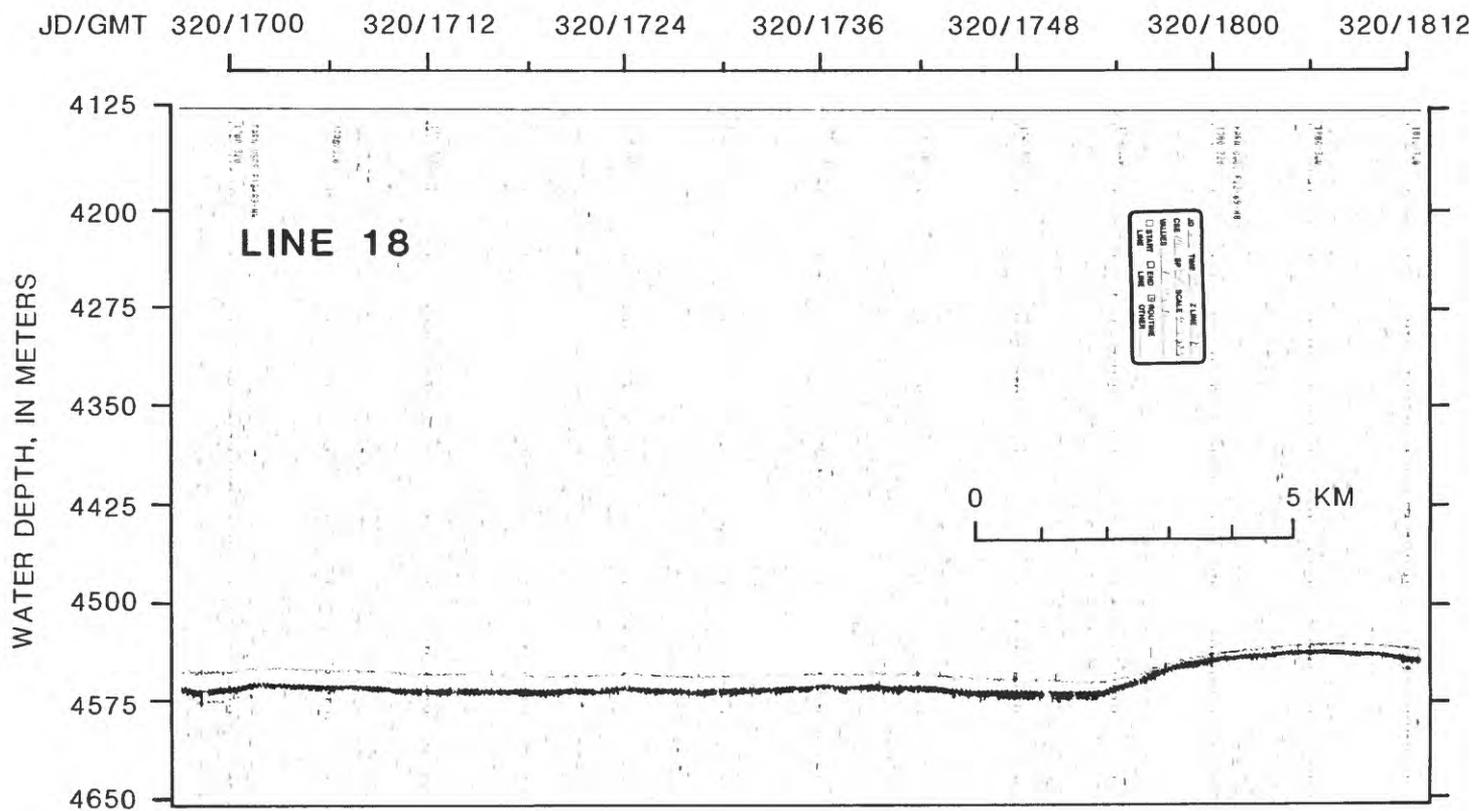
Figure 6b

Figure 6c

Figure 6d
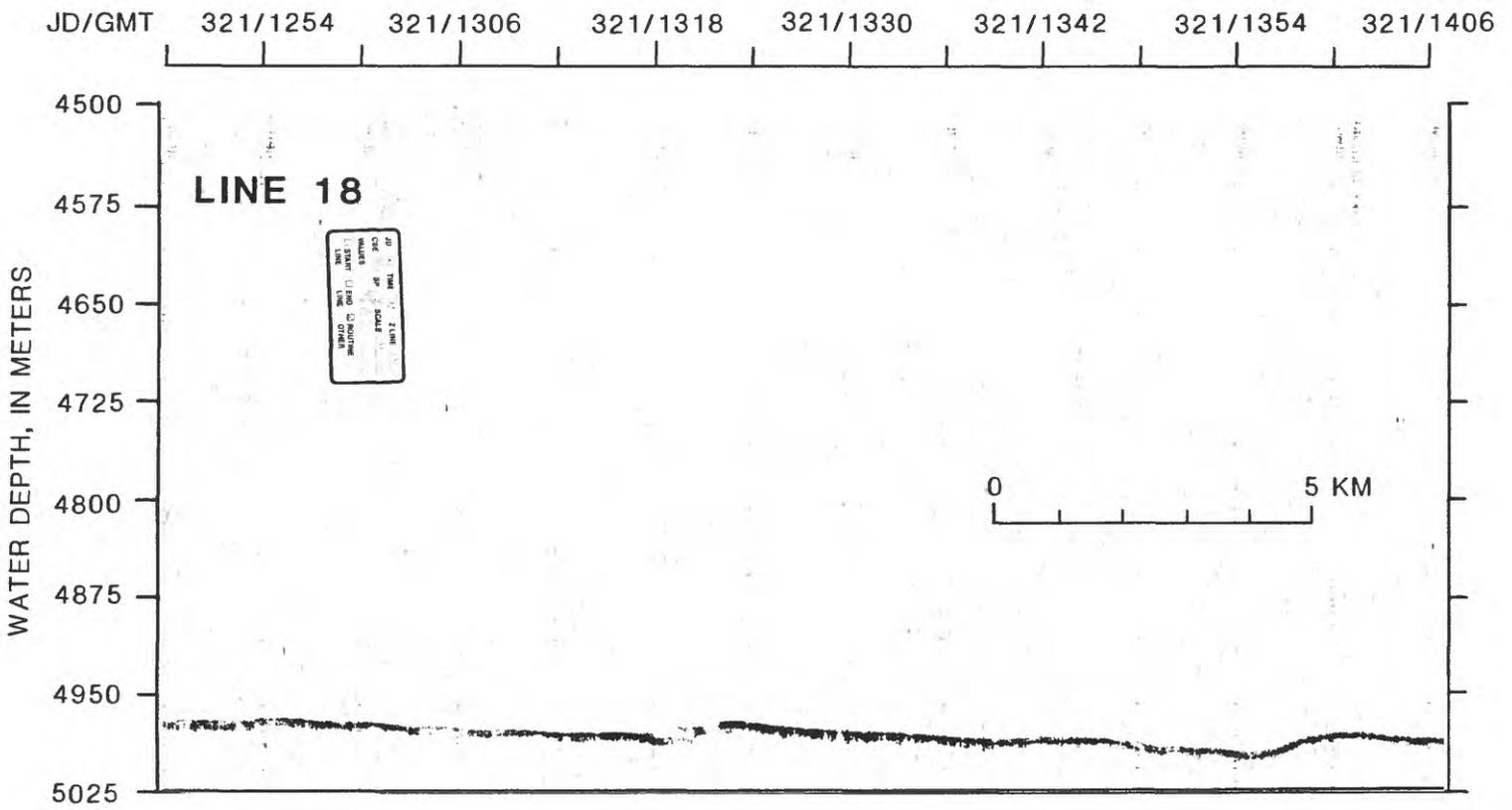
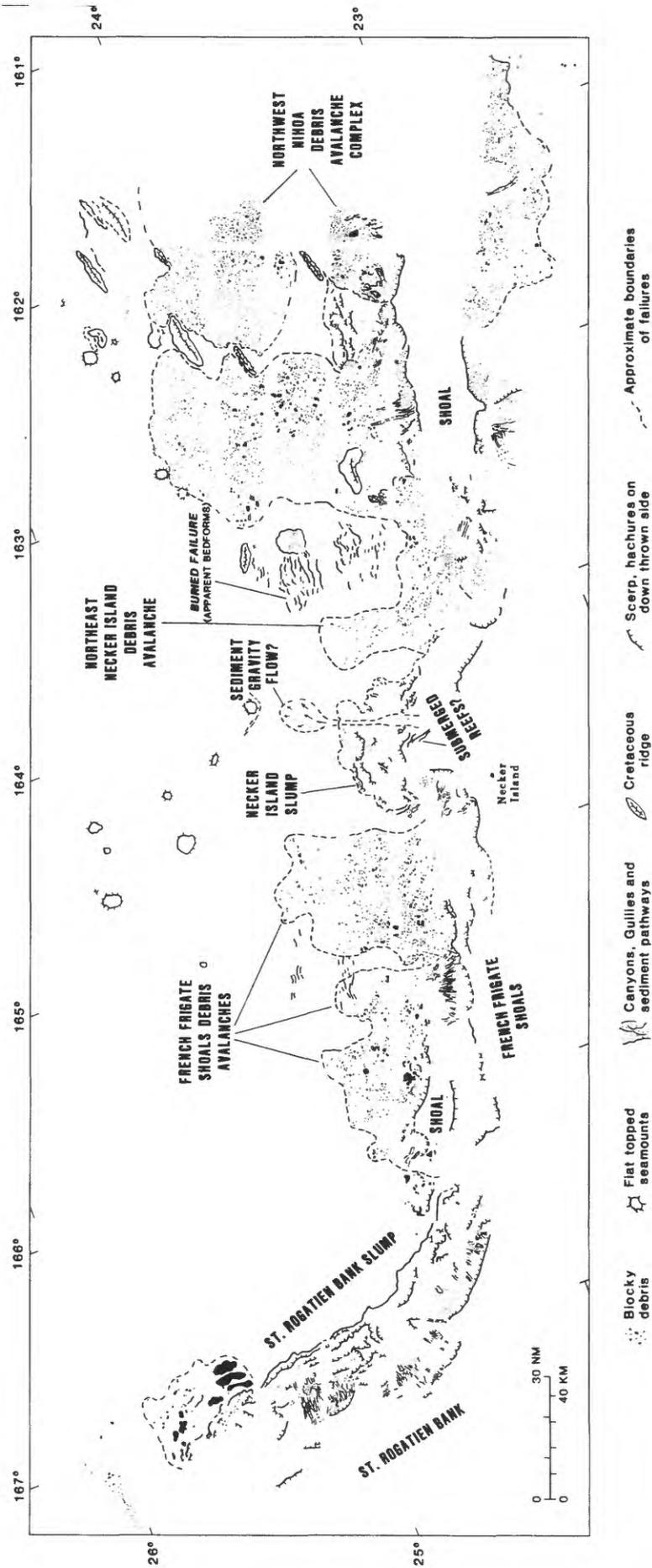Figure 6e
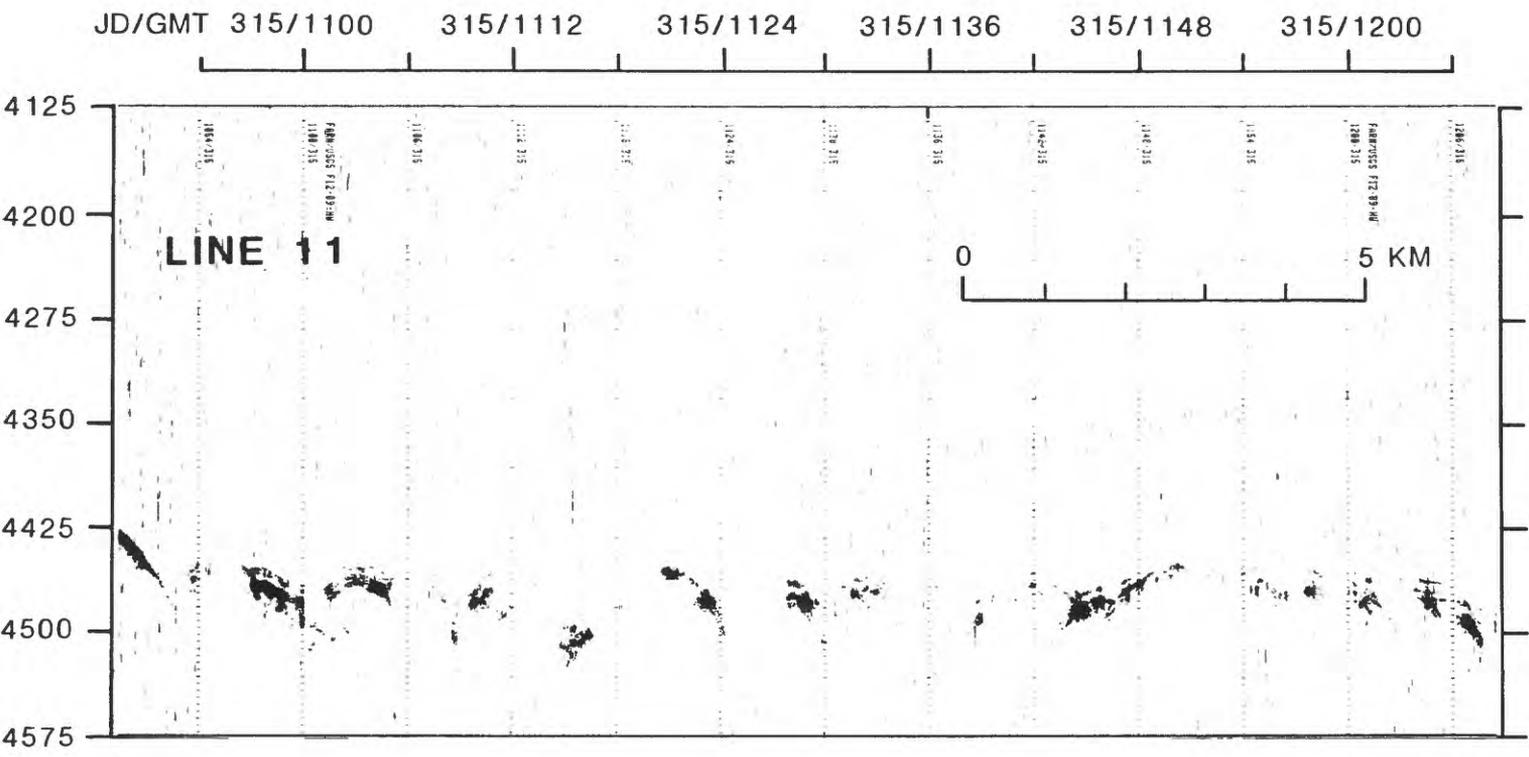
Figure 6f
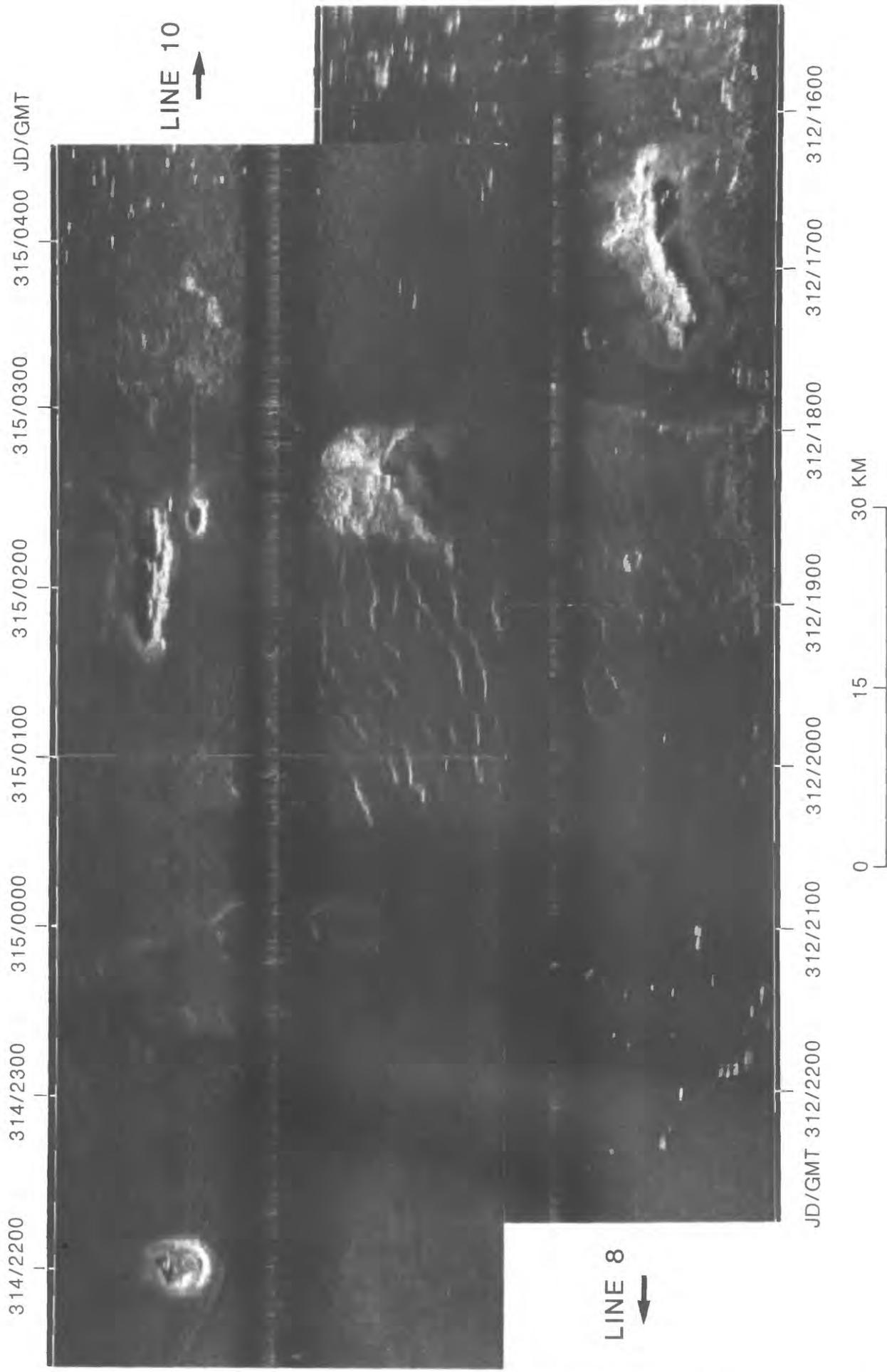
Figure 6g

Figure 6h

Figure 7a

Figure 7b

50

Figure 7c

Figure 8

53
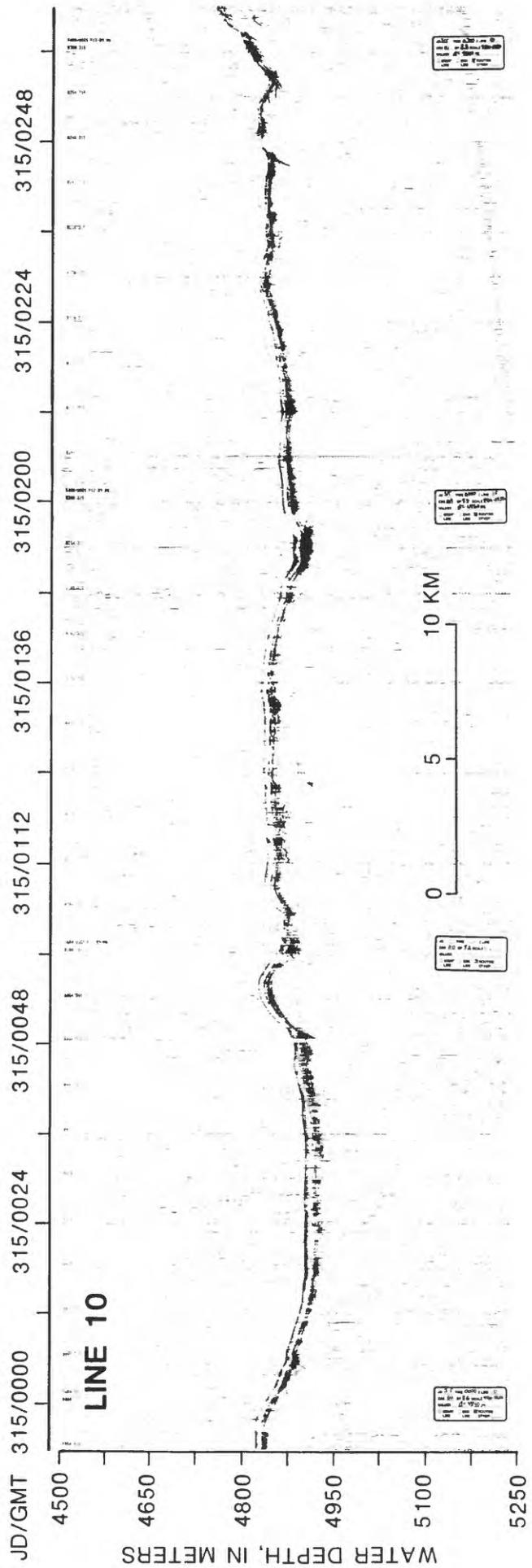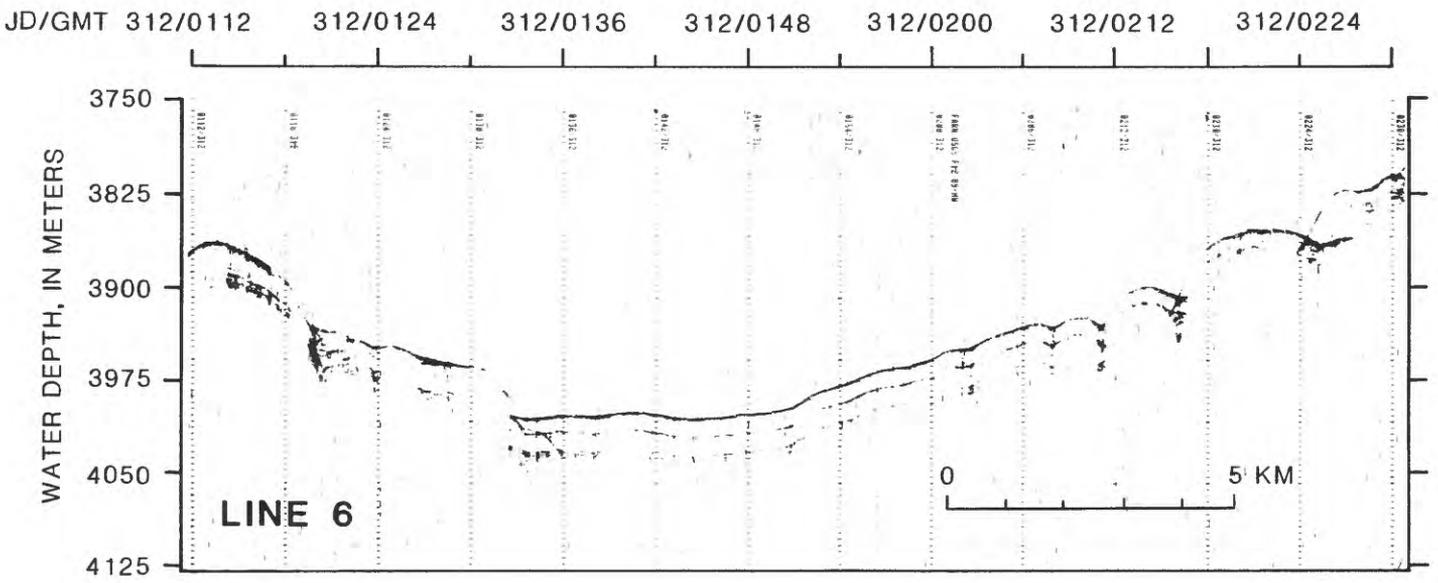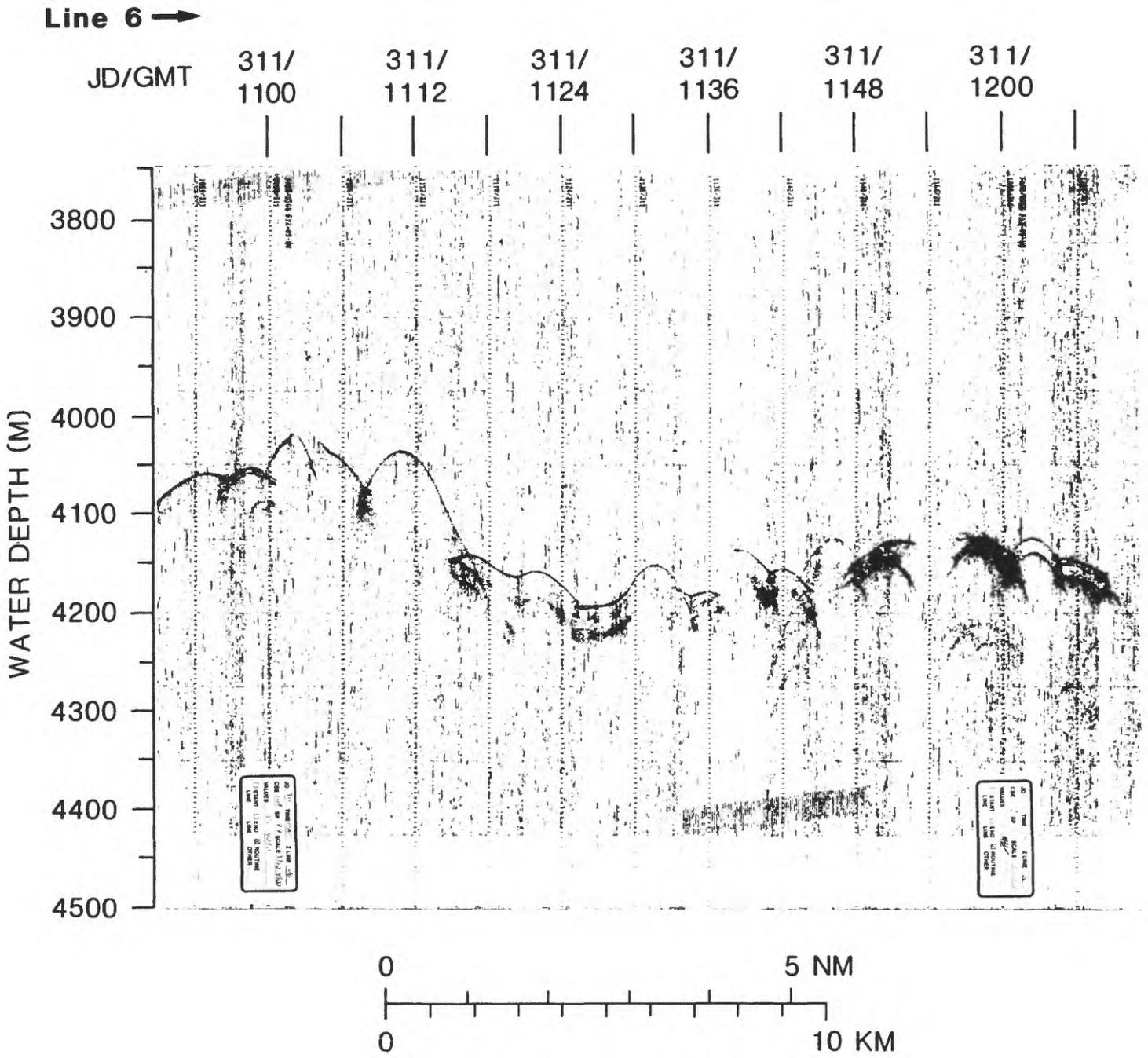
Figure 9a

Figure 9b

Figure 9c

55

Figure 9d

56

Figure 10

Line 8

Figure 11a

LINE 8

WATER DEPTH, IN METERS

0   10   20 KM
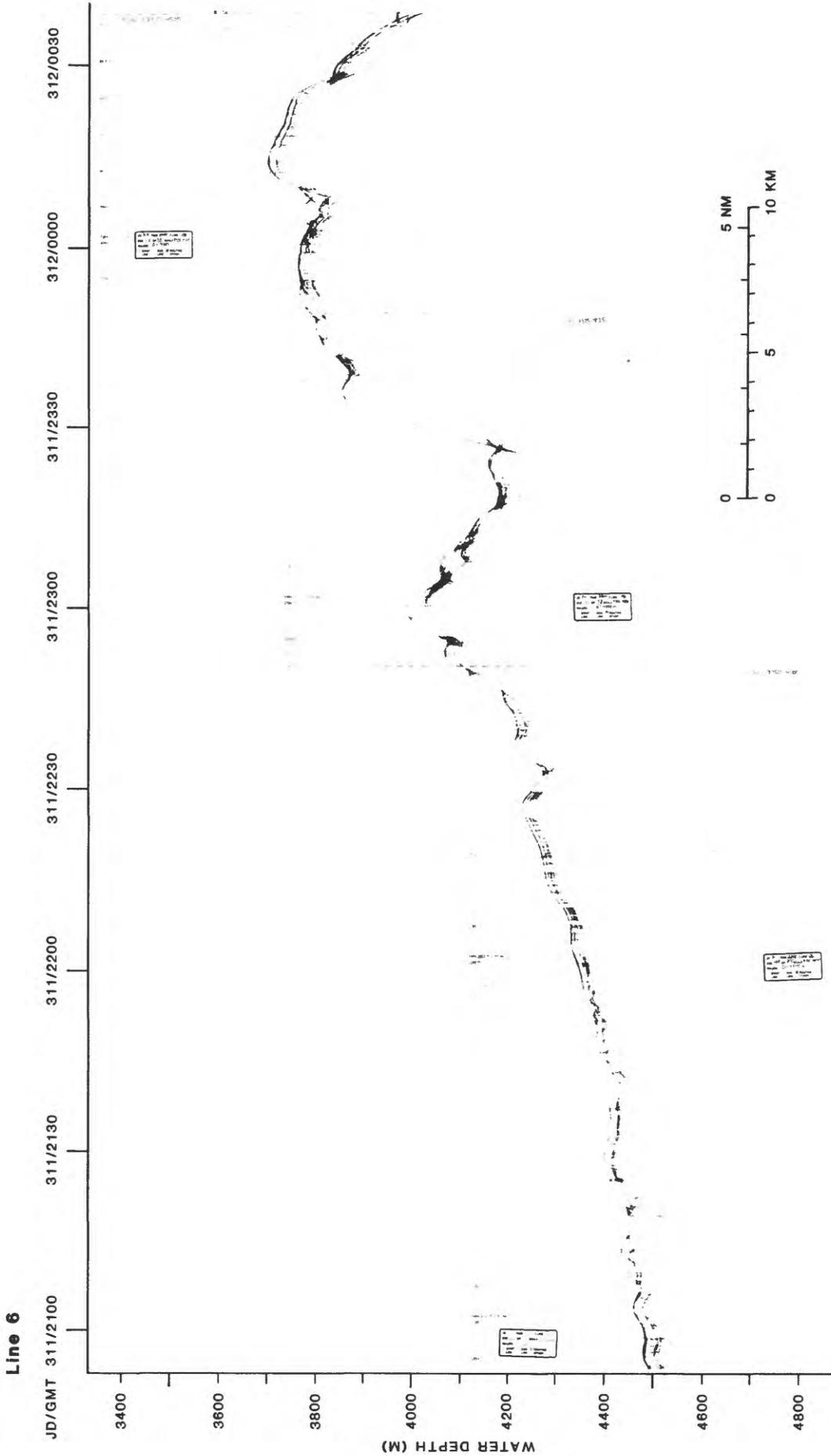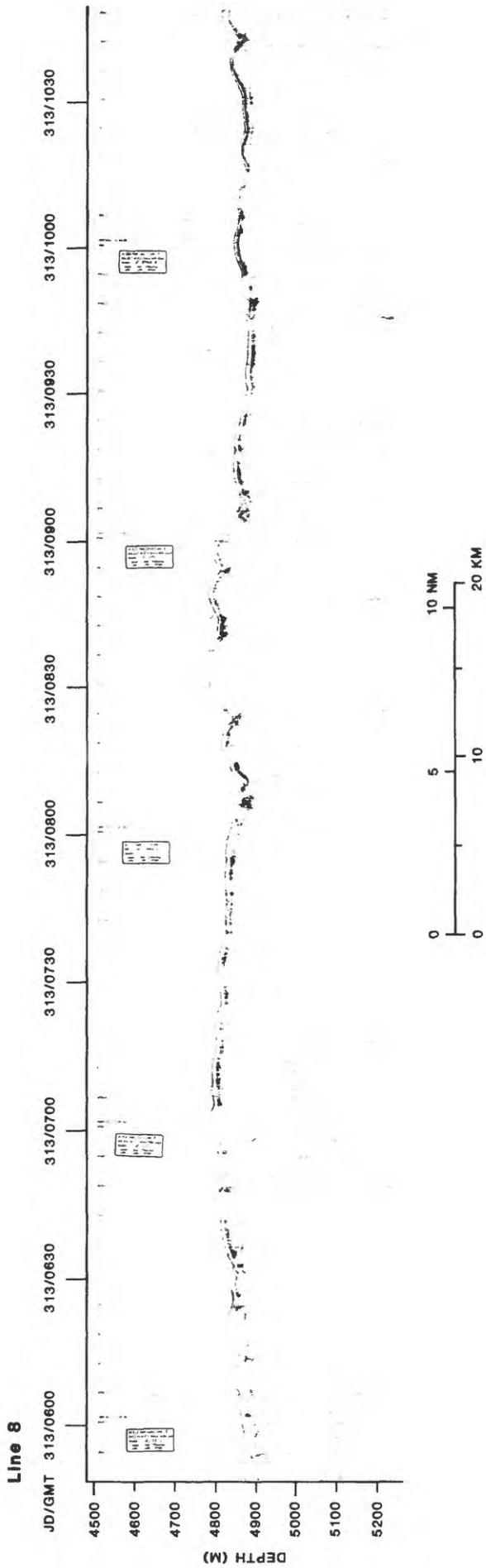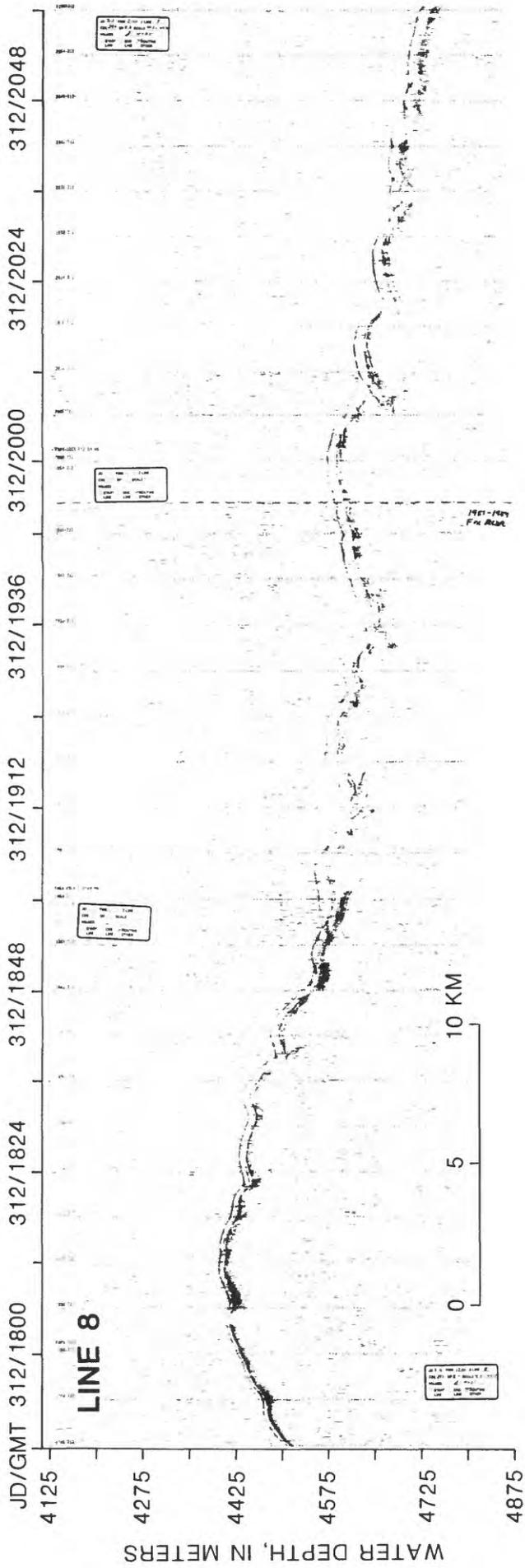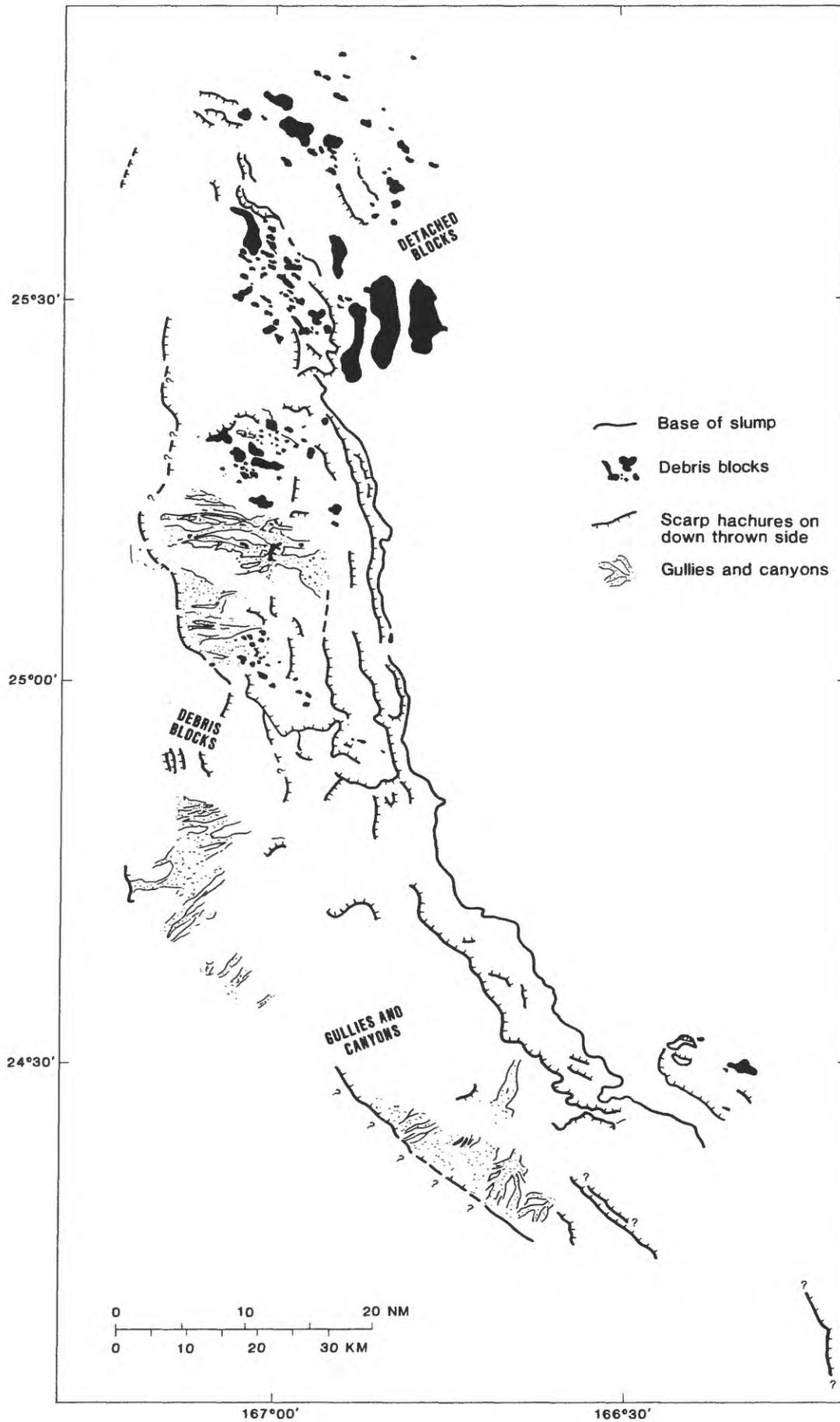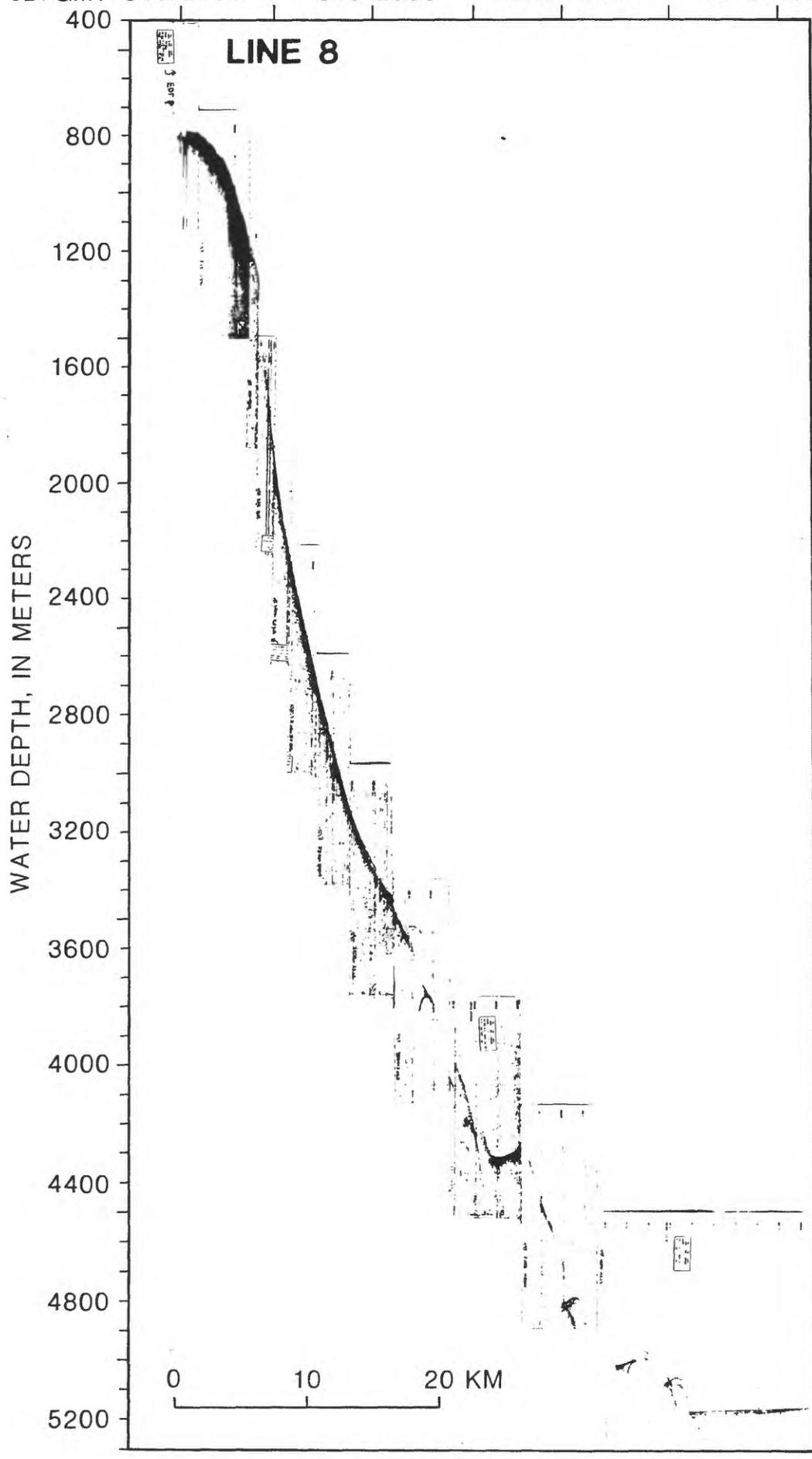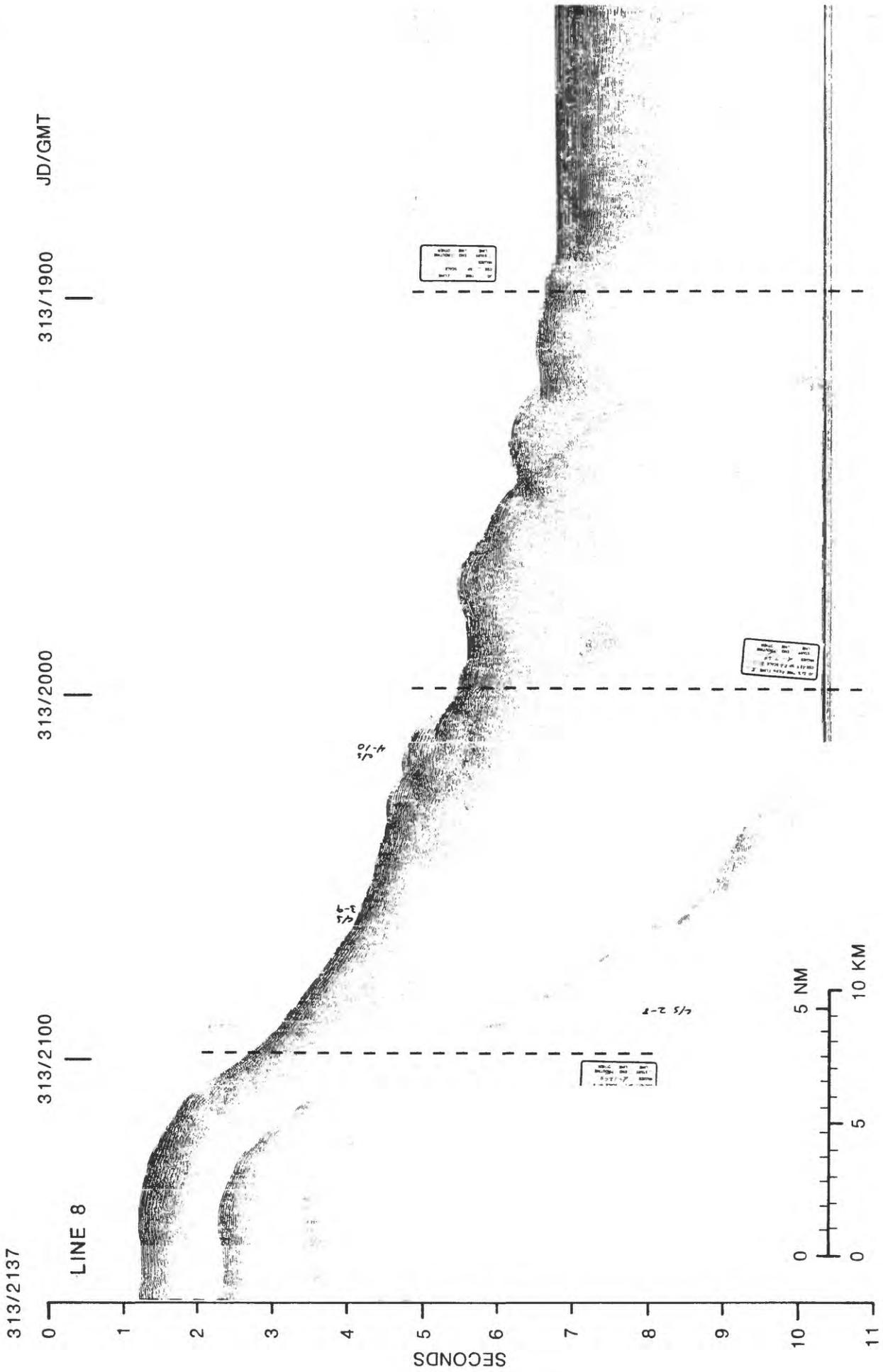
Figure 11b

Figure 11c

310/1700   310/1800   310/1900   310/2000

Line 5
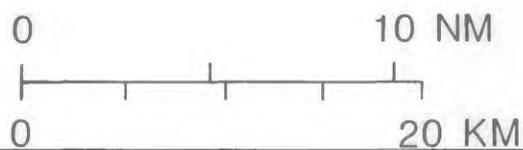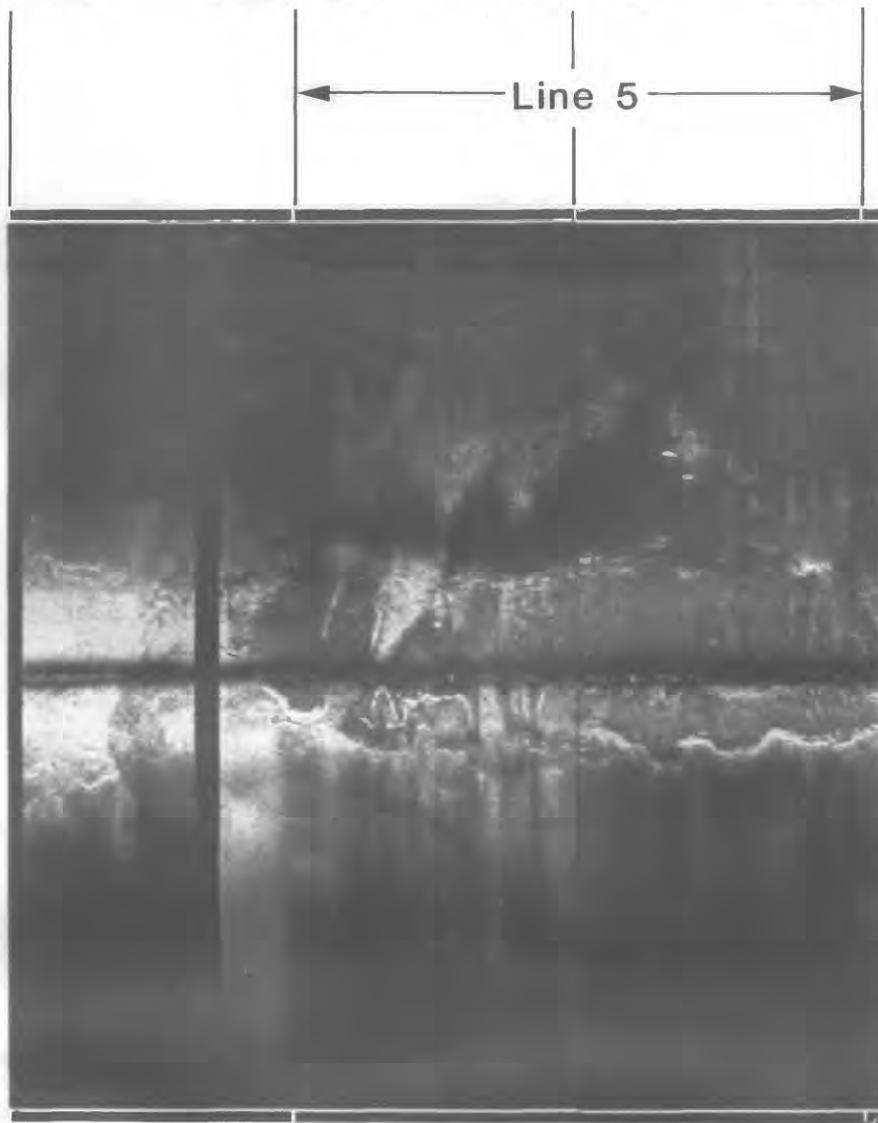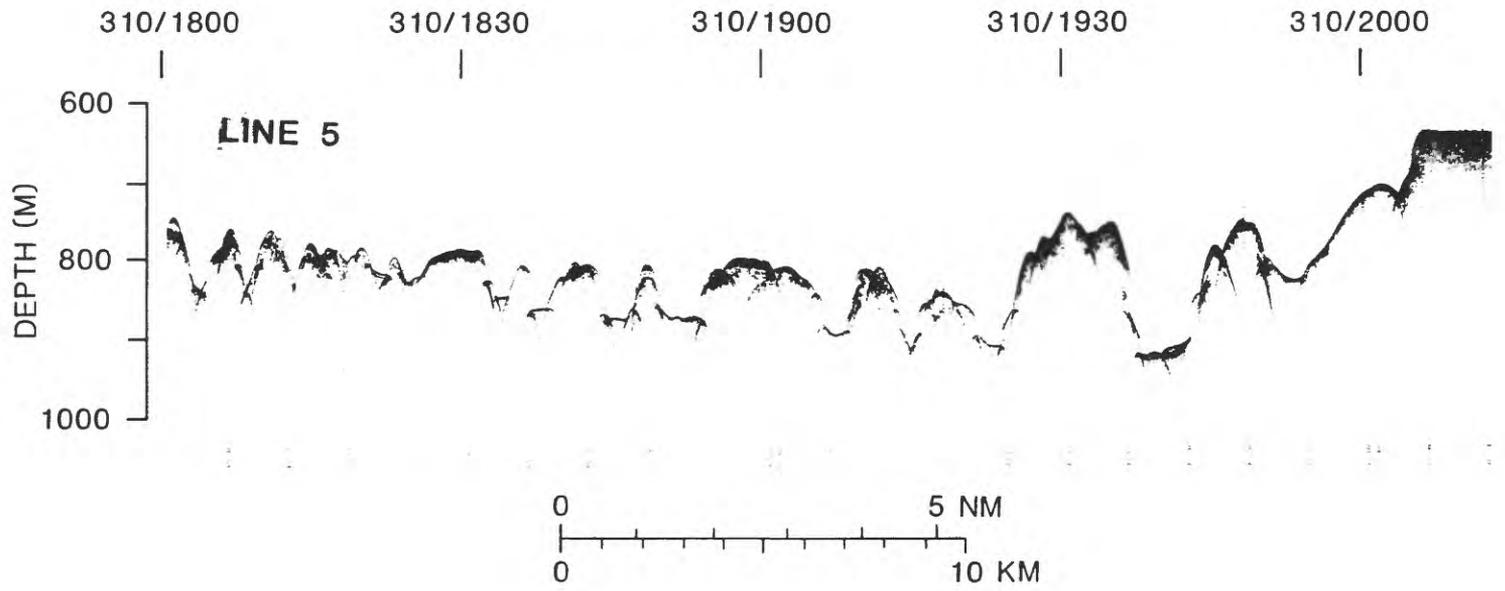
0   10 NM

0   20 KM

Figure 12a

Figure 12b

APPENDIX I

EQUIPMENT SETTINGS AND COMMENTS

3.5 kHz SYSTEM

LSR Recorder	Mode -	Continuous
		PAPER - 100 lpi
		SWEEP - 1 sec
		PROGRAM - As required
		GAIN - Mid
		CONTRAST - Mid
		THRESHOLD - Min

PTR Transceiver	GAIN - 6
	POWER - -6db
	PULSE WIDTH - Not used

IOS Correlator	OUTPUT LEVEL - 4-5
	ATTENUATOR - 11.5

Fish Depth Compensation	10 m.

10 Khz SYSTEM

MUFAX Recorder	ATTENUATOR - -6 to -18
	TIME MARKS - 6 min.
	PULSE LENGTH - 2.8 to 5
	FISH DEPTH - 2x5 m
	GATING SELECTOR - 6
	FATHOMS/METERS - Meters
	TRIGGER (Left/Center) -as required for scale changes
	TVG - Use to suppress outgoing pulse
	GATING - Use to "see" bottom through outgoing pulse

MAGNETOMETER/GRADIOMETER

Soltec Recorder

CHART SPEED - 40 cm/hr

All three channels at 100 gamma range

GRAVIMETER

Soltec Recorder

CHART SPEED - 10 cm/hr

SEISMIC REFLECTION SYSTEM

LSR Recorder

DISPLAY - Normal

STYLUS SCAN - 2 sec

PAPER - 120 lpi

MEMORY SWEEP - 6 sec

FILTER - out

POLARITY - +

GAIN 10 to 2 O'clock

CONTRAST -30 to -40

THRESHOLD - 2

Krohn - Hite Filter

20-120 Hz

Masscomp

GAIN SETTING: Pre-amp 0

Post-amp 6 to 18

DMD Delay Box

As required for DWD

APPENDIX 2: Summary of GLORIA Passes For F12-89-HW

TAPE	FILE	PASS	START TIME	END TIME
1	1	1	0108/309	0659/309
1	2	2	0700/309	1259/309
1	3	3	1300/309	1859/309
1	4	4	1900/309	0059/310
1	5	5	0100/310	0659/310
1	6	6	0700/310	1259/310
1	7	7	1300/310	1859/310
1	8	8	1900/310	0059/311
1	9	9	0100/311	0659/311
1	10	10	0700/311	1259/311
1	11	11	1300/311	1859/311
1	12	12	1900/311	0059/312
1	13	13	0100/312	0659/312
1	14	14	0700/312	1259/312
1	15	15	1300/312	1859/312
1	16	16	1900/312	0059/313
2	1	17	0100/313	0659/313
2	2	18	0700/313	1259/313
2	3	19	1300/313	1859/313
2	4	20	1900/313	0059/314
2	5	21	0100/314	0659/314
2	6	22	0700/314	1259/314
2	7	23	1300/314	1859/314
2	8	24	1900/314	0059/315
2	9	25	0100/315	0659/315
2	10	26	0700/315	1259/315
2	11	27	1300/315	1859/315
2	12	28	1900/315	0059/316
2	13	29	0100/316	0659/316
2	14	30	0700/316	1259/316
2	15	31	1300/316	1859/316

2	16	32	1900/316	0059/317
3	1	33	0100/317	0659/317
3	2	34	0700/317	1259/317
3	3	35	1300/317	1859/317
3	4	36	1900/317	0059/318
3	5	37	0100/318	0659/318
3	6	38	0700/318	1259/318
3	7	39	1300/318	1859/318
3	8	40	1900/318	0059/319
3	9	41	0100/319	0659/319
3	10	42	0700/319	1259/319
3	11	43	1300/319	1859/319
3	12	44	1900/319	0059/320
3	13	45	0100/320	0659/320
3	14	46	0700/320	1259/320
3	15	47	1300/320	1859/320
3	16	48	1900/320	0059/321
4	1	49	0100/321	0659/321
4	2	50	0700/321	1259/321
4	3	51	1300/321	1859/321
4	4	52	1900/321	0059/322
4	5	53	0100/322	0659/322
4	6	54	0700/322	1259/322
4	7	55	1300/322	1859/322
4	8	56	1900/322	0059/323
4	9	57	0100/323	0659/323
4	10	58	0700/323	1259/323
4	11	59	1300/323	1859/323
4	12	60	1900/323	0059/324
4	13	61	0100/324	0659/324
4	14	62	0700/324	1259/324
4	15	63	1300/324	1859/324
4	16	64	1900/324	0059/325
5	1	65	0100/325	0659/325
5	2	66	0700/325	1259/325
5	3	67	1300/325	1859/325

5	4	68	1900/325	0059/326
5	5	69	0100/326	0659/326
5	6	70	0700/326	1259/326
5	7	71	1300/326	1859/326
5	8	72	1900/326	0059/327
5	9	73	0100/327	0659/327
5	10	74	0700/327	1259/327
5	11	75	1300/327	1859/327
5	12	76	1900/327	0059/328
5	13	77	0100/328	0659/328
5	14	78	0700/328	1259/328
5	15	79	1300/328	1859/328
5	16	80	1900/328	2153/328